NIST Special Publication 260
NIST SP 260-261

Standard Reference Materials: SRM 1453a, Expanded Polystyrene Board for Thermal Conductivity from 282 K to 314 K

Jae Hyun Kim
Adam L. Pintar

This publication is available free of charge from:
https://doi.org/10.6028/NIST.SP.260-261

NATIONAL INSTITUTE OF STANDARDS AND TECHNOLOGY
U.S. DEPARTMENT OF COMMERCE

NIST Special Publication 260
NIST SP 260-261

Standard Reference Materials: SRM 1453a, Expanded Polystyrene board for Thermal Conductivity from 282 K to 314 K

Jae Hyun Kim
Engineering Laboratory
Building Energy and Environment Division

Adam L. Pintar
Information Technology Laboratory
Statistical Engineering Division

This publication is available free of charge from:
https://doi.org/10.6028/NIST.SP.260-261

March 2026

U.S. Department of Commerce
Howard Lutnick, Secretary

National Institute of Standards and Technology
Craig Burkhardt, Acting Under Secretary of Commerce for Standards and Technology and Acting NIST Director

NIST SP 260-261
March 2026

NIST Technical Series Policies

Publication History
Approved by the NIST Editorial Review Board on 2025-09-15

How to Cite this NIST Technical Series Publication
Kim JH, Pintar A. (2026) Standard Reference Materials: SRM 1453a, Expanded Polystyrene board for Thermal Conductivity from 282 K to 314 K. (National Institute of Standards and Technology, Gaithersburg, MD), NIST Special Publication (SP) NIST SP260-261. https://doi.org/10.6028/NIST.SP.260-261

Author ORCID iDs
Jae Hyun Kim: 0000-0003-2599-6062
Adam L Pintar: 0000-0002-5021-2576

Abstract

Thermal conductivity measurements at and near room temperature are presented as the basis for certified values of thermal conductivity for SRM 1453a, Expanded Polystyrene board. The measurements have been collected according to a statistically designed experiment using the NIST 1016 mm line-heat-source guarded-hot-plate apparatus. The thermal conductivities of the SRM specimens were measured over a bulk density range of 42 kg·m^{-3} to 54 kg·m^{-3} and a mean temperature range of 282 K to 314 K. Uncertainties for the measurements, consistent in format with current international guidelines, have been prepared. The physical properties of the SRM sample population were also statistically analyzed and the variations between boards are reported.

Each SRM 1453a specimen is individually certified for bulk density, ρ, and batch certified for thermal conductivity per the following equation:

$$\lambda = -0.12383 + 0.001328 \times T_m + 2.9376 \times 10^{-5} \times \rho - 3.9977 \times 10^{-6} \times T_m^2 + 4.3384 \times 10^{-9} \times T_m^3$$

where λ is the predicted thermal conductivity (W·m^{-1}·K^{-1}) and T_m is the mean temperature (K). This equation is valid over the bulk density and temperature ranges of 42 kg·m^{-3} to 54 kg·m^{-3} and 282 K to 314 K, respectively. The expanded uncertainty for λ from the above equation is 1.9 % with a coverage factor of k = 2.

Keywords

Calibration; bulk density; expanded polystyrene board; guarded-hot-plate apparatus; heat-flow-meter apparatus; standard reference material; SRM 1453a; thermal conductivity; thermal insulation; uncertainty

Table of Contents

List of Tables

List of Figures

Acknowledgments

The authors appreciate the comments and discussions with R. R. Zarr, retired from the National Institute of Standards and Technology and the assistance provided by T. L. Gervasio in conducting the mass and dimensional measurements for bulk density. The authors express appreciation for compressive resistance measurements provided by D. L. Hunston, and the initial sample selections and procurement provided by J. Pagliaro and J. W. Hettenhouser.

1. Introduction

The National Institute of Standards and Technology (NIST) issues Standard Reference Materials® (SRMs) for insulation materials having certified value assignments for thermal conductivity or thermal resistance. Thermal insulation SRMs are intended specifically for application in standardized steady-state measurement methods. SRMs are used by industry, academia, and government to verify or improve the accuracy of specific measurements. Thermal insulation SRMs, in particular, are used for checking guarded-hot-plate apparatus [1] and for calibrating heat-flow-meter apparatus [2]. In the United States, these SRMs can also assist insulation manufactures in complying with federal requirements for labeling and advertising of home insulation by providing traceability per the U.S. Federal Trade Commission's more commonly referenced R-value Rule [3].

Value assignments for thermal insulation SRMs are developed with the guarded-hot-plate method [4-6]. The method is considered an absolute measurement procedure because the resulting thermal transmission properties are determined directly from basic measurements of electrical power, temperature, length, and area. Essentially, the method establishes steady-state heat flow through flat homogeneous slabs – the surfaces of which are in contact with adjoining parallel boundaries (i.e., plates) maintained at constant temperatures. The steady-state heat transmission properties of the test specimen are determined by measuring the plate separation and geometric shape factor for the heat flow and using the Fourier heat conduction equation. Influence quantities such as plate clamping pressure, plate emittance, and ambient air temperature, among others, are controlled; while other quantities, such as ambient air pressure, are monitored during the measurement process.

The thermal transmission properties of thermal insulation SRMs are characterized as functions of bulk density and mean temperature. Since it is impractical to measure the thermal conductivity of every specimen, a statistical sampling procedure is used to select specific specimens from the material lot for testing in the guarded-hot-plate apparatus. It should be noted that a thermal insulation SRM unit issued to a customer has not been measured directly in a NIST guarded-hot-plate apparatus. The analysis of the thermal conductivity data of the sample sub-lot is used for certification of the SRM lot. These characterization processes are realized by batch certification. The benefit of batch certification is production of a large quantity of units that are economical and available on demand for several years. Consequently, the uncertainty statement for a thermal insulation SRM contains a component of uncertainty due to the material lot variability.

This report provides supplement documentation for the SRM 1453a Certification on the following topics:

- overview and historical background;
- standard terminology for reference materials, thermal insulation, and measurement uncertainty;
- certification project plan;
- measurement methods for the bulk density and thermal conductivity;
- uncertainty analysis; and,
- certification

2. Overview

The renewal process for SRM 1453a involves three major phases (Fig.1): 1) material acquisition; 2) batch certification by the NIST technical laboratory; and 3) distribution by the NIST Office of Reference Materials (ORM).

2.1. Project Definition and Scope for Intended Use

Standard Reference Material 1453a, like previous 1453 lots, is a semi-rigid, high-density, expanded polystyrene (EPS) board.

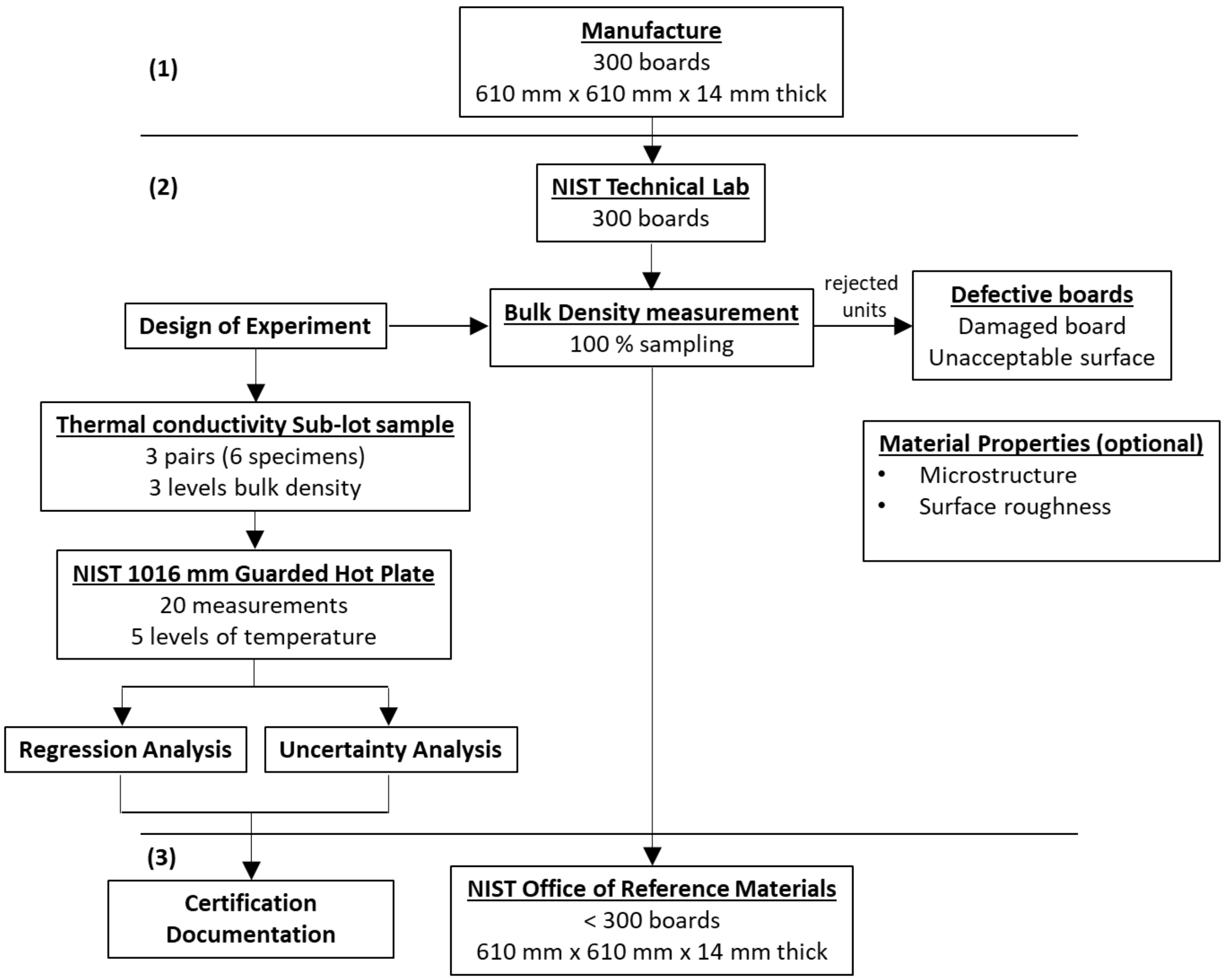

Fig. 1. Project plan for NIST SRM1453a, Expanded Polystyrene Board

2.2. Development and Production

In Phase 1, the NIST technical laboratory assesses the needs and priorities of U.S. industry with regard to thermal insulation reference materials. Based on industry input, the laboratory prepares the technical requirements for procurement of the insulating material. Execution of Phase 1 generally requires one year from initiation to completion.

In Phase 2, the technical lab proceeds with certification of the renewal after delivery of procured material. Sampling and measurement plans with statistical justification are developed as follows:

1) Measurements of bulk density for homogeneity screening of the material lot (100 % sampling) are carried out for the purpose of rejection of anomalous and/or damaged panels,

2) selection of a sub-sample of 6 pairs of specimens containing low (2 pair), mid (2 pair), and high (2 pair) bulk density levels, and

3) thermal conductivity measurements of a statistical sub-sample using the NIST 1016 mm guarded-hot-plate apparatus and analysis of data are carried out for batch certification.

In Phase 3, the NIST Office of Reference Materials (ORM) undertakes all final administrative functions including document review and approval, pricing, storage, shipping, publicity, and customer support. The production costs of the renewal are recovered, under current Congressional authorization, through the sale of the SRM to end users. Figure 1 outlines the project plan for the development and production of SRM 1453a, Expanded Polystyrene Board. Similar approaches illustrated in Fig. 1 have been followed in various SRM developments, including for SRM 1453.

2.3. Historical Progress

Standard Reference Material 1453a, like the previous 1453 lot, is a rigid, high-density, expanded polystyrene board commercially manufactured by PFB manufacturing LLC[1]. Table 1 reviews the chronology of the 1453 Series.

Table 1. Chronology of SRM 1453, expanded polystyrene board

SRM	Year acquired	Year issued	Bulk density ($kg{\cdot}m^{-3}$)	Temperature (K)	Ref.	NIST facility
1453	1994	1996[a]	37 to 46	281 to 313	[4]	b
1453a	2021	2025	42 to 54	282 to 314		b

[a] Original certificate date
[b] NIST 1016 mm diameter guarded-hot-plate apparatus, Gaithersburg, Maryland

[1] Certain equipment, instruments, software, or materials are identified in this paper in order to specify the experimental procedure adequately. Such identification is not intended to imply recommendation or endorsement of any product or service by NIST, nor is it intended to imply that the materials or equipment identified are necessarily the best available for the purpose

The planning and research phase for SRM 1453 began in 1994 when NIST acquired 300 boards of molded expanded polystyrene foam from the manufacturer. Surface imprints caused by molding of the individual boards were removed using a milling machine. The mean bulk density for SRM 1453 was 41 kg·m^{-3} and the vendor was required to trim the boards to a final panel size of 660 mm by 930 mm. The planning and research phase for SRM 1453a began in 2021 when NIST acquired 300 boards of expanded polystyrene foam from a manufacturer. Sanding of the individual boards were not needed since the individual boards were produced by heat wire cutting of a block of EPS without creating an unusual surface texture. The mean bulk density for SRM 1453a was 47 kg·m^{-3} and the vendor was required to trim the board to a final panel size of 610 mm by 610 mm.

2.4. Comparisons of 1453a and 1453

Microstructures and surface roughnesses of SRM 1453a were investigated to compare morphological characteristics with SRM 1453.

The microcellular structure of SRM 1453a was examined using scanning electron microscopy (SEM). A small section of SRM 1453a was cut from one board using a razor blade and sputter-coated with gold to avoid surface charging. SEM images at magnifications of 25× and 100× are shown in Fig. 2a and 2b, respectively. Similarly, SRM 1453 was also examined for comparison purposes. Fig. 2a shows the fused beads of expanded polystyrene from the molding process. The individual beads were forming a foam structure defined by interfaces between the beads. The size of the beads measured at longest distance ranged from approximately 1 mm to 2 mm and the voids were frequently observed at intersection of multiple beads. Fig. 2b shows the detailed cell structures formed within the individual beads. The structures of the cells were elliptical in shape, and the size of the cells measured along the major axis were mostly smaller than 0.1 mm. A large percentage of the cell walls were intact indicating a relatively high content of closed cells. The shapes of the microstructures of SRM1453a were comparable with SRM 1453 while the cell sizes of SRM 1453a were smaller than those of SRM 1453.

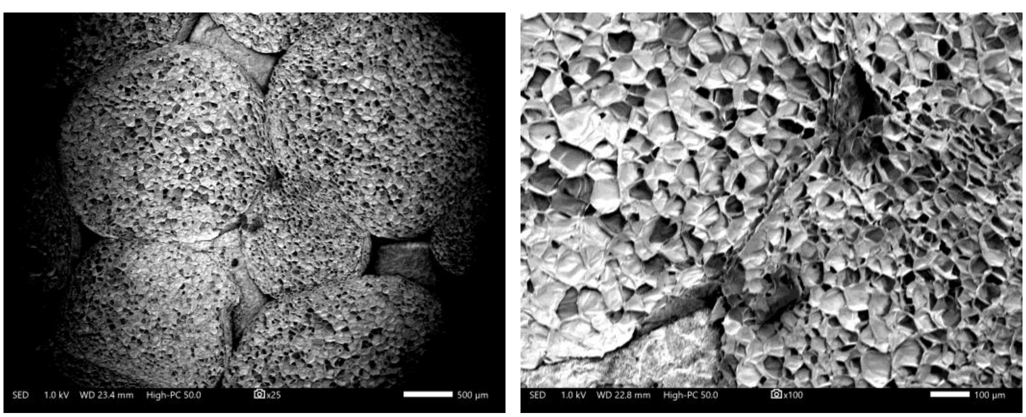

(a) (b)

Fig. 2. SEM images of (a) molded beads and internal cellular structure at 25 × and (b) enlarged cellular structure at 100 × for SRM 1453a sample.

The surface roughness of SRM 1453a board was examined by NIST Sensor Science Division using a stylus profilometer instrument (Form Talysurf PGI 1240). Nine (9) line profiles on the surface of a small square section (127 mm by 128 mm) were obtained by travelling the 2 µm radius of the stylus tip along 22.5 mm of evaluation length. The roughness average (R_a) for the unsanded surface was 24.2 µm with the combined uncertainty of ± 3.8 µm (k = 2), and those for the sanded surface were 17.0 µm and ± 4.1 µm (k = 2) respectively. The difference in the R_a values for the unsanded and sanded samples were statistically insignificant. Furthermore, the difference in the R_a values for SRM 1453a was significantly smaller than that of SRM 1453 before and after sanding, indicating that no improvement of the surface flatness was needed for the SRM 1453a. Therefore, SRM 1453a boards were not sanded.

Table 2. Roughness average values for expanded polystyrene boards

Sample ID	Roughness average, R_a (µm)	
	Unsanded	Sanded
1453	72 to 82	16 to 20
1453a	24.2	17.0

3. Terms and Definitions

3.1. Reference Materials

Section 3.1 provides definitions for reference materials, excerpted verbatim, from Refs. [7, 8].

Reference Material (RM): Material, sufficiently homogeneous and stable with respect to one or more specified properties, which has been established to be fit for its intended use in a measurement process [8]. NOTE: RM is a generic term, and properties can be quantitative or qualitative, e.g. identity of substances or species. Uses may include the calibration of a measurement system, assessment of a measurement procedure, assigning values to other materials, and quality control. ISO/IEC Guide 99:2007 has an analogous definition (5.13), but restricts the term "measurement" to apply to quantitative values. However, Note 3 of ISO/IEC Guide 99:2007, 5.13 (VIM) specifically includes qualitative properties, called "nominal properties".

Certified Reference Material (CRM): Reference material (RM) characterized by a metrologically valid procedure for one or more specified properties, accompanied by an RM certificate that provides the value of the specified property, its associated uncertainty, and a statement of metrological traceability [8]. NOTE: The concept of value includes a nominal property or a qualitative attribute such as identity or sequence. Uncertainties for such attributes may be expressed as probabilities or levels of confidence. Metrologically valid procedures for the production and certification of RMs are given in, among others, ISO Guides 34 and 35. ISO Guide 31 gives guidance on the contents of RM certificates. ISO/IEC Guide 99:2007 has an analogous definition (5.14).

NIST Standard Reference Material® (SRM): A CRM issued by NIST that also meets additional NIST-specified certification criteria and is issued with a certificate or certificates of analysis that reports the results of its characterizations and provides information regarding the appropriate use(s) of the material [7]. NOTE: A SRM is prepared and used for three main purposes: (1) To help develop accurate methods of analysis; (2) to calibrate measurement systems used to facilitate exchange of goods, institute quality control, determine performance characteristics, or measure a property at the state-of-the-art limit; and (3) to ensure the long-term adequacy and integrity of measurement quality assurance pro-grams. The terms "Standard Reference Material" and the diamond-shaped logo which contains the term "SRM," are registered with the United States Patent and Trademark Office.

NIST Certified Value: A value reported on an SRM certificate or certificate of analysis for which NIST has the highest confidence in its accuracy in that all known or suspected sources of bias have been fully investigated or accounted for by NIST [7].

3.2. Thermal Insulation

Section 3.2 provides terms, symbols, definitions, and units pertaining to properties and measurements of thermal insulating materials, excerpted verbatim, from Refs. [1] and [9].

apparent thermal conductivity, λ_a or k_a: a thermal conductivity assigned to a material that exhibits thermal transmission by several modes of heat transfer resulting in property variation with specimen thickness, or surface emittance (SI units: $(W{\cdot}m^{-2}) / (K{\cdot}m^{-1}) = W{\cdot}m^{-1}{\cdot}K^{-1}$) [9].

NOTE 1 Thermal conductivity and resistivity are normally considered to be intrinsic or specific properties of materials and, as such, should be independent of thickness. When nonconductive modes of heat transfer are present within the specimen (radiation, free convection) this may not be the case. To indicate the possible presence of these phenomena (for example, thickness effect) the modifier “apparent” is used, as in apparent thermal conductivity.

NOTE 2 Test data using the “apparent” modifier must be quoted only for the conditions of the measurement. Values of thermal conductance and thermal resistance calculated from apparent thermal conductivity or resistivity, are valid only for the same conditions.

density, ρ: the mass per unit volume of material. (SI units: $kg{\cdot}m^{-3}$) [9].

NOTE 1 The metered section density, ρ_m, or the specimen density, ρ_s where metered section area density cannot be obtained, are to be reported as the average of the two pieces (excerpted from Ref. [1]). The equation for specimen density is the following:

$$\rho_S = \frac{m_S}{A_S \times L} \qquad (1)$$

where:
m_s = mass of the specimen (kg),
A_s = area of the specimen (m^2), and
L = specimen thickness (m).

heat flow; heat flow rate, Q: the quantity of heat transferred to or from a system in unit time (W) [9].

NOTE 1 This definition is different from that given in some textbooks, which may use $\dot{Q}$ or $\dot{q}$ to represent heat flow rate. The ISO definition uses Φ.

heat flux, q: the heat flow rate through a surface of unit area perpendicular to the direction of heat flow ($W{\cdot}m^{-2}$) [9].

fibrous (fiber) glass: a synthetic vitreous fiber insulation made by melting predominantly silica sand and other inorganic materials, and then physically forming the melt into fibers [9].

NOTE 1 To form an insulation product, there are often other materials applied to the fibrous glass such as binders, oils, etc.

thermal conductivity, λ: the time rate of steady state heat flow through a unit area of a homogeneous material induced by a unit temperature gradient in a direction perpendicular to that unit area (SI units: $(W \cdot m^{-2}) / (K \cdot m^{-1}) = W \cdot m^{-1} \cdot K^{-1}$) [9].

NOTE 1 Thermal conductivity testing is usually done in one of two apparatus/specimen geometries: flat-slab specimens with parallel heat flux lines, or cylindrical specimens with radial heat flux lines. The operational definition of thermal conductivity for flat-slab specimens is given as follows:

$$\lambda = \frac{QL}{A\Delta T} \quad (2)$$

where:
Q = heat flow rate,
A = area through which Q passes, and
L = thickness of the flat-slab specimen across which the temperature difference ΔT exists
The *ΔT/L* ratio approximates the temperature gradient.

thermal resistance, *R*: the quantity determined by the temperature difference, at steady state, between two defined surfaces of a material or construction that induces a unit heat flow rate through a unit area.

$$R = \frac{\Delta T}{q} = \frac{L}{\lambda} \quad (3)$$

A resistance (*R*) associated with a material shall be specified as a material *R*. A resistance (*R*) associated with a system or construction shall be specified as a system *R* (R in SI units: $K / (W \cdot m^{-2}) = K \cdot m^2 \cdot W^{-1}$) [9]

NOTE 1 Thermal resistance and thermal conductance are multiplicative reciprocals.

thermal transmission properties: those properties of a material or system that define the ability of a material or system to transfer heat such as thermal resistance and thermal conductivity, among others [1].

semi-rigid board insulation: qualitative property associated with the degree of suppleness (i.e., flexibility), particularly related to the geometrical dimensions and bulk density of the board.

3.3. Uncertainty

Section 3.3 provides definitions pertaining to measurement uncertainty from Refs. [10, 11].

combined standard uncertainty, u_c: standard uncertainty of the result of a measurement when that result is obtained from the values of a number of other quantities, equal to the positive square root of a sum of terms, the terms being the variances or covariances of these other quantities weighted according to how the measurement result varies with changes in these quantities.

coverage factor, *k*: numerical factor used as a multiplier of the combined standard uncertainty in order to obtain an expanded uncertainty.

NOTE 1 A coverage factor, k, is typically in the range 2 to 3.

expanded uncertainty, *U*: quantity defining an interval about the result of a measurement that may be expected to encompass a large fraction of the distribution of values that could be reasonably attributed to the measurand.

standard uncertainty, u_i: uncertainty of the result of a measurement expressed as standard deviation.

Type A evaluation (of uncertainty): method of evaluation of uncertainty by the statistical analysis of a series of observations

Type B evaluation (of uncertainty): method of evaluation of uncertainty by means other than the statistical analysis of a series of observations

4. Certification Project Design

Section 4 describes the project plan for certification of SRM 1453a beginning with the project definition and scope for intended use. Brief descriptions of the material and fabrication processes are presented. The material preparation at NIST covers inspection, storage, and conditioning as part of the overall sampling plan. Lastly, the measurement methods for the homogeneity analysis, certification measurements, and uncertainty evaluation are described.

4.1. Project Definition and Scope for Intended Use

The certification project is defined as follows:

> The preparation of thermal insulation SRM 1453a (47 kg·m^{-3}) for thermal conductivity and thermal resistance measurements with expanded uncertainties (k = 2) associated with the certified values of less than or equal to 2 % over a mean temperature range of 282 K to 314 K.

Standard Reference Material 1453a is intended for use as a proven check for the guarded-hot-plate apparatus [1], or other absolute thermal conductivity apparatus, and for calibration of a heat-flow-meter apparatus [2] over the temperatures 282 K to 314 K. This report cannot exclude the use of SRM 1453a for other purposes, but the user is cautioned that other applications are not necessarily covered by the SRM 1453a Certificate or by this report.

4.2. Material and Fabrication

SRM1453a is a commercial rigid expanded polystyrene board with the mean bulk density of 47 kg·m^{-3}. The material lot was manufactured and fabricated in board form by PFB manufacturing LLC. The typical dimensions of the finished boards are 610 mm by 610 mm with a nominal thickness of 14 mm.

4.3. Delivery, Inspection, and Storage

The individual boards having a nominal size of 610 mm by 610 mm were shipped to the NIST Gaithersburg campus in October 2021. Visual inspections for individual panels were performed and an identification number from 1 to 300 was sequentially assigned to each panel using a handheld printer in black on one edge. The material lot was stored in a laboratory workspace under ambient conditions.

4.4. Measurement methods

The densities of the entire lot of material were measured. The results of the study were used to select a sub-sample for the thermal characterization of the reference material.

4.4.1. Sampling Procedure

The 300 panels were divided into 12 groups of 25 panels. Each group of 25 panels was placed in the lab at ambient conditions of 24 °C for a minimum 40 hours before starting the mass and dimensional measurements by two operators.

4.4.2. Bulk Density

The bulk density was determined for each panel from gravimetric and dimensional measurement procedures. The objective of the bulk density study was to assess the homogeneity of the lot between insulation boards (i.e. material variability), thereby providing empirical data for the following:

- Quantitative ranking of the material lot by bulk density
- The upper and lower bulk density limits of the material lot
- Detection of any anomalous thermal insulation boards for possible exclusion

4.4.3. Thermal Characterization

The steady-state thermal transmission measurements were determined in accordance with ASTM Test Method C177 using the NIST 1016 mm guarded-hot-plate apparatus. The thermal conductivity of SRM 1453a was batch certified. Sub-sampling of the insulation material lot was based on a similar approach taken for the development of the previous version, SRM 1453. The SRM 1453a lot was sub-sampled at three levels of bulk density (low, mid, and high). Quantitative values for these rankings were defined using the results of the homogeneity study.

5. Bulk Density Study

This section describes the mass and dimensional measurements, graphical analyses, and tabulated results for mass, panel area, thickness, and bulk density for the insulation panels. The mass and dimensions of the individual boards were randomly measured by two operators in a laboratory under ambient conditions of approximately 24 °C and 20 % to 45 % relative humidity. The measurements for all 300 boards (acquired in 12 groups of 25 boards) were conducted over 63 days from April 25, 2023 to June 26, 2023. The following data were collected for the 300 boards.

- 2700 mass measurements (9 observations per board × 300 boards)
- 648 lateral board dimensions (2 observations per board × 288 boards + 6 per board × 12 boards)
- 1248 thickness measurements (4 observations per board × 288 boards + 8 per board × 12 boards)

5.1. Mass Measurements

The mass of a specimen board was measured by gravimetry. The measurement station consisted of:

- Digital weighing balance (32.1 kg range, 0.0001 kg resolution)
- Foot switch for manual activation of recording
- RS-232 serial interface for the digital balance and a desktop computer

The start time was synchronized with placement and removal of the specimen on the balance by using a foot switch. The mass data in kilograms were repeatedly acquired from the digital balance every 5 s for 45 s using a computer program. Thus, 9 mass measurements are recorded for each panel, denoted by m_{ij}, $j = 1, \ldots, 9$ and $i = 1, \ldots, 300$.

5.2. Lateral Panel Dimensional Measurements – Length and Width

Figure 3 illustrates the essential features of the measurement station for the lateral dimensions of a panel. The insulation panel was placed on the granite surface plate (1.2 m by 1.8 m, unilateral flatness tolerance of 0.020 mm, see Table 4 for calibration information) in a vertical position and clamped securely between an aluminum sheet and a right-angle support fixture. The fixture consisted of an aluminum jig plate (14 mm thick by 560 mm by 560 mm) attached to two right angles (200 mm by 125 mm). The right angles were precision ground square to within 0.051 mm (per 150 mm) and parallel to within 0.006 mm (per 150 mm). The touch probe (3 mm diameter carbide ball contact point, 0.4 N measuring force) was contacted on a round polished gage block placed on the insulation board. After establishing a zero-reference plane for the workpiece, the measurement process was checked at the beginning and end of the process, using a 609.6 mm gage standard consisting of two 304.8 mm gage blocks combined together. The linear dimensions, l_1, l_2, l_3 were measured by moving the height gage along the surface plate and contacting the workpiece. Afterwards, the panel was unclamped and rotated 90°, and re-clamped to measure l_4, l_5, l_6. In each group, two middle locations (l_2 and l_5) of 24 boards were measured, and one board was selected for measurements at all locations (l_1, l_2, l_3, l_4, l_5, and l_6). It is necessary to measure some lateral dimension multiple times so that within board variability and measurement error may be estimated separately from between board variability.

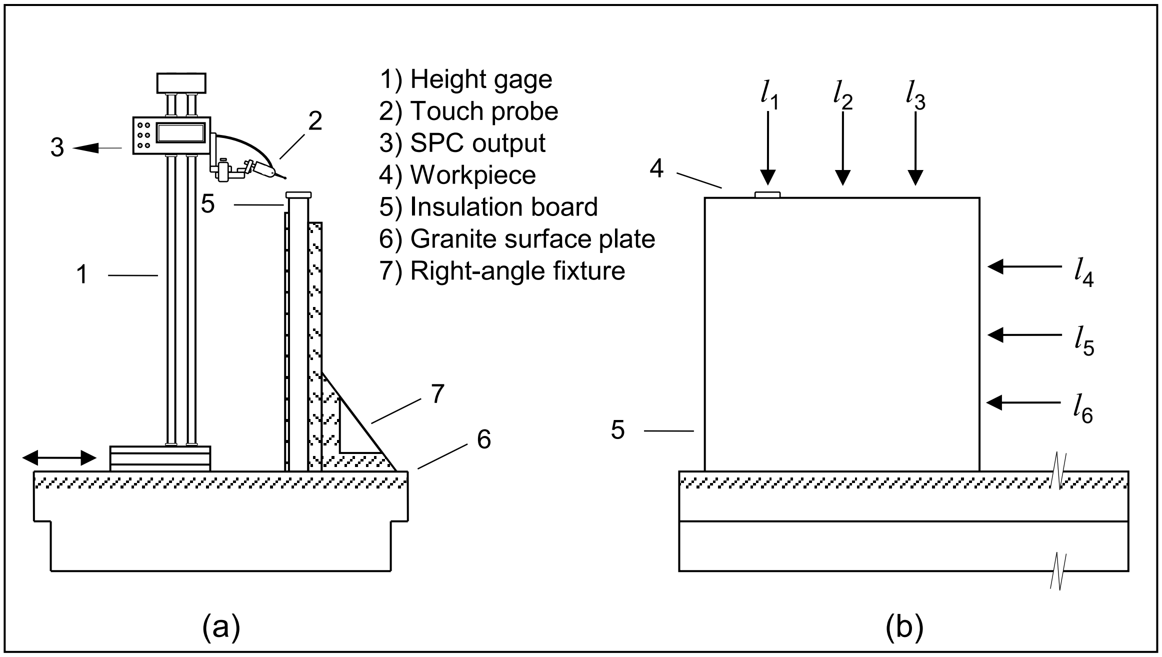

Fig. 3. (a) Side view of height gage and right-angle fixture with insulation board clamped between the aluminum jig plate and aluminum sheet. (b) Front view of panel length measurement at locations l_1.

Let $l_{ij}^{(123)}$ represent measurements of l_1, l_2, or l_3 ($j = 1, 2$, or 3) from board $i = 1, \ldots, 300$, and let $l_{ij}^{(456)}$ represent measurements of l_4, l_5, or l_6 ($j = 1, 2$, or 3) from board $i = 1, \ldots, 300$. For boards where only l_2 and l_5 are measured, j is always 1. For boards where measurements are recorded at all three locations, $j = 1, 2, 3$.

5.3. Thickness

Figure 4 illustrates the essential features of the configuration for the thickness measurements of a board. The measurements were made on the same surface plate as the lateral dimension measurements but using a different height gage (330 mm range, 0.01 mm resolution, 0.4 N measuring force), computer, and SPC (statistical process control) data output cable with converter tool to USB (Universal Serial Bus) cable. The board was placed horizontally on the granite surface plate (Fig.4a), and 8 metallic rings (outer diameter 70 mm, inner diameter 44 mm, thickness 13 mm) with a mean mass of 0.2636 (kg) ± 0.0001 (kg) were placed on the locations of the thickness measurements to ensure contact between the board and surface plate. After establishing a zero-reference plane for the workpiece, the measurement process was checked at the beginning and end of the process, using a 14 mm gage block (see Table 4 for calibration information). For the thickness measurements, the height gage was stationary, and the panel re-positioned so that the touch probe contacted the workpiece at each measurement location. For each group, one-half of the boards were measured at the corners (*L_1*, *L_3*, *L_5*, and *L_7*) and the other half were measured at the mid-centers (*L_2*, *L_4*, *L_6*, and *L_8*). As a check, one panel from each group was selected for measurements at locations *L_1* through *L_8*.

Let L_{ij} represent thickness measurement j on board $i = 1, \ldots, 300$. For the boards only measured at locations L_1, L_3, L_5, and L_7, or L_2, L_4, L_6, and L_8, $j = 1, \ldots, 4$, but for the boards measured at all 8 location, $j = 1, \ldots, 8$.

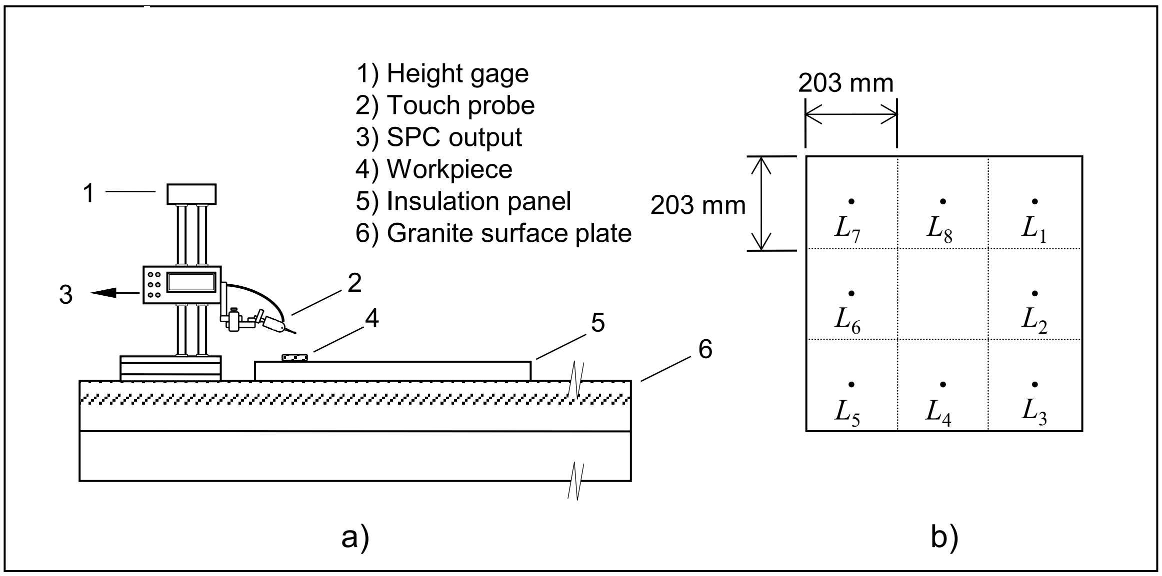

Fig. 4. (a) Front view shows 305 mm height gage and insulation board with workpiece on granite surface plate. (b) Top view shows the 8 measurement locations (*L_1* through *L_8*) each in the geometric center of a 203 mm by 203 mm subdivision of the insulation board (metallic rings are not shown).

5.4. Density Measurements

The gravimetric and dimensional measurements are jointly statistically modeled using a multivariate random effects model. Modeling the gravimetric and dimensional measurements jointly is important so that positive correlations between them may be captured, e.g., a thicker panel may also have more mass. This statistical model yields a predicted value for each panel for each dimensional measurement and the gravimetric measurement as well as statements of uncertainty about those predicted values in the form of probability distributions. The uncertainty in the predicted values originates from making only a small number of measurements on each board, different locations for the dimensional measurements and a finite amount of time for the gravimetric measurements.

Let $l_i^{(123)}$ be the predicted value for board $i = 1, \ldots, 300$ along the lateral dimension measured by the l_1, l_2, and l_3 locations. Similarly, let $l_i^{(456)}$ be the predicted value for board $i = 1, \ldots, 300$

along the lateral dimension measured by the l_4, l_5, and l_6 locations. Let L_i be predicted value for the thickness of board $i = 1, \dots, 300$, and m_i be the predicted value for mass measurement of board $i = 1, \dots, 300$. The measurement of bulk density for board $i = 1, \dots, 300$ is given by the measurement equation in Eq. (4)

$$\rho_{b,i} = \frac{(m_i + B_m)}{(l_i^{(123)} + B_l^{(123)}) \times \left(l_i^{(456)} + B_l^{(456)}\right) \times (L_i + B_L)} \qquad (4)$$

where B_m, $B_l^{(123)}$, $B_l^{(456)}$ and B_L represent mean zero additive errors with the standard uncertainty of the errors evaluated by Type B methods. The standard uncertainty of $B_l^{(123)}$ and $B_l^{(456)}$ is 0.077 mm from Table A1.1 of Appendix 1; the standard uncertainty of B_L is 0.038 mm from Table A1.1 of Appendix 1; and the standard uncertainty of B_m is 0.0001 kg from Section A1.1.

5.4.1. Tabulated Results

Table 3 summarizes the physical properties of Board IDs 002 to 301 (300 boards) and includes the quantities: mass (average of 9 measurements), length (l_2 or the average of l_1, l_2, and l_3), width (l_5 or the average of l_4, l_5, and l_6), area ($l_2 \times l_5$), thickness (average of 4 or 8 measurements), bulk density (from Eq. 4), and the combined standard uncertainty of the bulk density (from Eq. 4). The bulk densities listed in Table 3 may not be exactly equal to the obvious calculation from the other columns of Table 3 because predicted values from the random effects model are listed in the bulk density column. The standard uncertainty varies between panels because some panels are measured more times than others and because the non-linear nature of Eq. (4) requires that the uncertainty associated with each panel depends on the predicted values of each dimension and mass.

Table 3. Physical properties of SRM 1453a units (300 boards)

Board ID	Mass (kg)	Length (mm)	Width (mm)	Area (m^2)	Thickness (mm)	Bulk density ($kg \cdot m^{-3}$)	Bulk density from Eq.4 ($kg \cdot m^{-3}$)	Bulk density standard uncertainty ($kg \cdot m^{-3}$)
002	0.23371	608.37	608.23	0.37003	13.75	45.93	45.92	0.39
003	0.24050	608.56	607.88	0.36993	14.46	44.96	44.98	0.36
004	0.23137	608.51	607.27	0.36953	14.08	44.48	44.47	0.37
005	0.23277	608.42	607.36	0.36953	14.27	44.15	44.16	0.36
006	0.25152	608.19	608.60	0.37014	14.64	46.42	46.45	0.37
007	0.24241	608.21	608.01	0.36980	14.03	46.73	46.72	0.39
008	0.23506	607.59	608.24	0.36956	14.37	44.28	44.29	0.36
009	0.25821	608.58	608.42	0.37027	14.55	47.93	47.94	0.38
010	0.25803	607.91	608.38	0.36984	14.71	47.43	47.45	0.37
011	0.24854	607.87	608.47	0.36987	14.14	47.54	47.53	0.39

Board ID	Mass (kg)	Length (mm)	Width (mm)	Area (m^2)	Thickness (mm)	Bulk density ($kg{\cdot}m^{-3}$)	Bulk density from Eq.4 ($kg{\cdot}m^{-3}$)	Bulk density standard uncertainty ($kg{\cdot}m^{-3}$)
012	0.23108	608.09	607.83	0.36962	14.25	43.87	43.89	0.36
013	0.23571	608.14	607.87	0.36967	14.50	43.98	44.01	0.35
014	0.24079	607.83	607.79	0.36943	14.54	44.84	44.86	0.36
015	0.23693	607.78	607.96	0.36951	14.28	44.91	44.92	0.37
016	0.24979	608.50	608.86	0.37049	14.29	47.20	47.22	0.38
017	0.25784	608.51	608.34	0.37018	14.56	47.84	47.85	0.38
018	0.24991	608.54	608.35	0.37021	14.09	47.91	47.90	0.4
019	0.24318	607.96	608.43	0.36990	14.09	46.67	46.67	0.39
020	0.23161	607.80	608.34	0.36975	13.80	45.40	45.39	0.38
021	0.24323	608.01	608.47	0.36996	14.09	46.65	46.65	0.39
022	0.25251	608.03	608.48	0.36997	14.58	46.82	46.84	0.37
023	0.24146	608.01	608.56	0.37001	13.90	46.94	46.93	0.39
024	0.25310	608.06	608.45	0.36998	14.57	46.96	46.96	0.36
025	0.24559	607.83	608.27	0.36972	14.67	45.29	45.32	0.38
026	0.23449	607.79	608.21	0.36966	13.93	45.53	45.52	0.37
027	0.24509	607.78	608.19	0.36965	14.60	45.43	45.45	0.39
028	0.23523	607.78	608.15	0.36962	13.93	45.68	45.66	0.36
029	0.24218	607.88	607.98	0.36958	14.11	46.46	46.44	0.35
030	0.25056	607.90	608.32	0.36980	14.55	46.56	46.57	0.36
031	0.26118	609.39	608.16	0.37061	13.77	51.19	51.14	0.37
032	0.24983	609.08	607.87	0.37024	14.86	45.42	45.46	0.38
033	0.23260	609.13	607.91	0.37030	13.71	45.82	45.82	0.38
034	0.26407	608.34	608.20	0.36999	14.70	48.54	48.55	0.40
035	0.24547	608.20	608.16	0.36988	14.00	47.42	47.41	0.39
036	0.25798	608.44	608.24	0.37008	14.67	47.53	47.54	0.38
037	0.24846	608.48	608.54	0.37028	14.11	47.56	47.56	0.39
038	0.24060	607.89	608.51	0.36991	14.06	46.26	46.26	0.37
039	0.24891	607.90	608.31	0.36979	14.55	46.27	46.28	0.39
040	0.24276	607.75	608.28	0.36968	14.59	45.02	45.04	0.36
041	0.22937	607.78	608.29	0.36971	13.71	45.26	45.24	0.38
042	0.24640	607.46	607.77	0.36920	14.68	45.47	45.48	0.37
043	0.22826	607.71	607.85	0.36940	14.02	44.08	44.08	0.39
044	0.23757	607.45	608.06	0.36937	14.56	44.18	44.20	0.36
045	0.22732	607.75	607.95	0.36948	13.87	44.36	44.36	0.35
046	0.24004	607.74	608.15	0.36960	14.62	44.43	44.46	0.36
047	0.23940	607.83	608.37	0.36979	14.04	46.11	46.11	0.37
048	0.24932	607.80	608.28	0.36971	14.59	46.23	46.25	0.37
049	0.25227	607.78	609.16	0.37024	13.64	49.94	49.94	0.40

Board ID	Mass (kg)	Length (mm)	Width (mm)	Area (m^2)	Thickness (mm)	Bulk density ($kg·m^{-3}$)	Bulk density from Eq.4 ($kg·m^{-3}$)	Bulk density standard uncertainty ($kg·m^{-3}$)
050	0.27664	607.86	609.28	0.37036	15.01	49.78	49.81	0.39
051	0.26543	607.60	608.93	0.36999	14.82	48.42	48.43	0.38
052	0.24839	607.64	609.08	0.37010	13.74	48.84	48.81	0.41
053	0.26911	607.66	609.17	0.37017	14.95	48.64	48.68	0.38
054	0.24759	608.12	608.49	0.37003	13.90	48.14	48.11	0.40
055	0.26271	608.33	608.29	0.37004	14.76	48.11	48.12	0.38
056	0.25193	608.45	608.22	0.37007	14.08	48.34	48.33	0.40
057	0.23084	607.48	609.45	0.37023	13.89	44.91	44.93	0.38
058	0.24189	607.52	609.34	0.37019	14.58	44.82	44.87	0.36
059	0.23347	607.49	609.27	0.37013	14.01	45.02	45.05	0.37
060	0.24532	607.67	608.88	0.37000	13.72	48.32	48.29	0.41
061	0.27379	607.85	609.11	0.37025	14.80	49.96	49.97	0.39
062	0.25859	607.89	609.29	0.37038	13.86	50.38	50.35	0.42
063	0.25144	607.77	609.34	0.37034	13.71	49.54	49.51	0.42
064	0.27336	607.76	609.09	0.37018	14.90	49.55	49.57	0.39
065	0.27662	607.89	608.90	0.37014	14.83	50.39	50.39	0.40
066	0.23650	607.86	609.94	0.37076	13.63	46.79	46.80	0.40
067	0.24962	607.69	609.28	0.37025	13.73	49.11	49.09	0.41
068	0.27046	607.74	609.26	0.37027	14.90	49.04	49.06	0.38
069	0.23350	607.66	609.73	0.37051	13.94	45.22	45.25	0.38
070	0.24162	607.60	609.56	0.37037	14.50	44.99	45.04	0.36
071	0.25531	608.73	610.29	0.37150	13.91	49.40	49.42	0.41
072	0.24771	609.67	608.26	0.37084	14.32	46.65	46.68	0.38
073	0.23303	609.34	608.01	0.37048	13.71	45.89	45.89	0.39
074	0.24092	607.69	609.41	0.37034	14.45	45.03	45.04	0.34
075	0.22924	609.19	607.75	0.37024	13.81	44.84	44.84	0.38
076	0.23629	609.11	607.69	0.37015	14.47	44.11	44.14	0.36
077	0.22696	609.02	607.71	0.37011	13.87	44.22	44.23	0.37
078	0.24671	607.69	609.85	0.37060	14.56	45.74	45.79	0.36
079	0.26921	608.49	609.34	0.37078	13.67	53.10	53.05	0.45
080	0.29208	609.23	609.31	0.37121	14.95	52.64	52.65	0.41
081	0.26586	608.59	609.50	0.37094	13.61	52.66	52.61	0.45
082	0.28648	608.48	609.45	0.37084	14.75	52.39	52.40	0.42
083	0.26521	607.70	609.52	0.37041	14.91	48.04	48.08	0.38
084	0.24712	607.59	609.45	0.37030	13.78	48.44	48.42	0.41
085	0.27181	607.86	609.22	0.37032	14.83	49.49	49.51	0.39
086	0.25692	607.74	609.22	0.37025	13.92	49.84	49.81	0.42
087	0.23582	608.92	607.58	0.36997	14.48	44.03	44.06	0.36

Board ID	Mass (kg)	Length (mm)	Width (mm)	Area (m^2)	Thickness (mm)	Bulk density ($kg \cdot m^{-3}$)	Bulk density from Eq.4 ($kg \cdot m^{-3}$)	Bulk density standard uncertainty ($kg \cdot m^{-3}$)
088	0.25729	609.23	608.02	0.37042	13.65	50.88	50.82	0.43
089	0.28100	609.24	608.11	0.37048	14.95	50.74	50.75	0.39
090	0.26534	608.90	607.74	0.37005	14.84	48.31	48.32	0.38
091	0.23964	608.20	608.62	0.37016	13.89	46.63	46.62	0.39
092	0.24591	607.98	608.43	0.36991	14.32	46.42	46.42	0.38
093	0.26304	608.71	609.52	0.37102	14.04	50.49	50.48	0.42
094	0.24577	607.67	609.49	0.37037	13.77	48.19	48.18	0.41
095	0.27878	609.43	607.72	0.37036	14.72	51.15	51.14	0.41
096	0.25250	607.86	608.91	0.37013	13.78	49.51	49.48	0.42
097	0.27146	608.79	607.81	0.37003	14.95	49.07	49.08	0.38
098	0.24840	608.76	607.83	0.37002	13.65	49.18	49.13	0.42
099	0.26858	608.86	607.96	0.37017	14.92	48.63	48.63	0.35
100	0.24627	608.91	607.85	0.37013	13.64	48.78	48.73	0.42
101	0.24924	608.04	609.04	0.37032	14.17	47.51	47.51	0.39
102	0.27261	608.83	608.31	0.37036	14.66	50.20	50.20	0.40
103	0.22694	607.49	607.26	0.36890	14.38	42.79	42.80	0.35
104	0.22172	607.56	607.25	0.36894	14.01	42.90	42.89	0.36
105	0.23214	607.60	607.22	0.36895	14.50	43.41	43.42	0.35
106	0.25360	607.62	608.21	0.36956	14.67	46.79	46.79	0.37
107	0.24506	607.59	608.27	0.36958	14.12	46.97	46.95	0.39
108	0.25314	607.71	608.29	0.36966	14.55	47.08	47.09	0.38
109	0.24639	607.71	608.25	0.36964	14.12	47.20	47.18	0.39
110	0.25341	607.68	608.21	0.36960	14.53	47.20	47.20	0.38
111	0.24432	607.73	608.24	0.36965	13.92	47.49	47.47	0.40
112	0.26704	608.31	609.45	0.37073	13.89	51.88	51.85	0.43
113	0.28508	608.27	609.47	0.37072	14.87	51.73	51.74	0.40
114	0.26747	608.31	609.47	0.37075	13.86	52.05	52.02	0.44
115	0.28778	608.37	609.39	0.37073	14.92	52.04	52.05	0.41
116	0.22093	607.16	607.87	0.36907	13.90	43.06	43.05	0.36
117	0.25223	607.80	609.30	0.37033	14.91	45.67	45.73	0.36
118	0.24310	609.42	608.00	0.37053	14.55	45.08	45.13	0.36
119	0.22873	609.23	607.93	0.37037	13.84	44.61	44.63	0.38
120	0.24347	607.85	608.92	0.37013	14.59	45.08	45.13	0.36
121	0.24551	607.77	609.30	0.37031	14.69	45.12	45.18	0.36
122	0.23417	607.81	608.92	0.37011	13.97	45.30	45.31	0.38
123	0.23273	607.75	609.39	0.37036	13.83	45.45	45.46	0.38
124	0.27850	608.07	609.19	0.37043	14.95	50.29	50.30	0.36
125	0.25394	608.12	609.20	0.37047	13.73	49.94	49.92	0.42

Board ID	Mass (kg)	Length (mm)	Width (mm)	Area (m^2)	Thickness (mm)	Bulk density ($kg·m^{-3}$)	Bulk density from Eq.4 ($kg·m^{-3}$)	Bulk density standard uncertainty ($kg·m^{-3}$)
126	0.27593	608.18	609.16	0.37048	14.92	49.92	49.94	0.39
127	0.25573	608.29	609.34	0.37066	13.70	50.37	50.34	0.43
128	0.27890	609.41	608.38	0.37075	14.94	50.34	50.37	0.39
129	0.25649	608.22	609.46	0.37069	13.63	50.77	50.73	0.43
130	0.28192	609.09	608.27	0.37049	15.00	50.74	50.75	0.39
131	0.25756	608.33	609.40	0.37072	13.57	51.20	51.15	0.44
132	0.28501	608.33	609.38	0.37070	15.04	51.11	51.13	0.40
133	0.26226	608.31	609.40	0.37070	13.77	51.39	51.35	0.43
134	0.23518	607.32	607.99	0.36924	14.41	44.21	44.23	0.36
135	0.23202	607.44	609.47	0.37022	13.74	45.63	45.64	0.39
136	0.24836	607.47	609.13	0.37003	14.83	45.27	45.31	0.36
137	0.23126	607.69	608.08	0.36952	14.07	44.49	44.50	0.37
138	0.23518	607.77	607.88	0.36945	13.84	46.00	45.97	0.39
139	0.23192	607.49	608.99	0.36996	13.83	45.32	45.32	0.38
140	0.28419	609.37	608.35	0.37071	14.90	51.45	51.46	0.40
141	0.26687	607.99	607.98	0.36965	13.78	52.38	52.29	0.44
142	0.26471	607.91	609.45	0.37049	13.90	51.41	51.38	0.43
143	0.28430	607.92	609.42	0.37048	14.90	51.52	51.53	0.40
144	0.26333	607.89	609.40	0.37045	13.67	52.02	51.96	0.44
145	0.28853	608.00	609.53	0.37059	15.01	51.87	51.88	0.40
146	0.25413	608.06	610.01	0.37092	14.39	47.62	47.66	0.38
147	0.26118	608.67	610.90	0.37184	13.91	50.51	50.54	0.42
148	0.25339	607.75	609.38	0.37035	13.60	50.32	50.28	0.43
149	0.27980	607.80	609.12	0.37022	15.06	50.20	50.20	0.36
150	0.26389	607.84	609.45	0.37045	13.96	51.05	51.02	0.42
151	0.28112	607.86	607.87	0.36950	14.84	51.29	51.25	0.41
152	0.25253	608.01	609.40	0.37052	13.73	49.63	49.61	0.42
153	0.25528	608.32	609.15	0.37056	13.70	50.29	50.26	0.43
154	0.26574	602.35	609.35	0.36704	14.53	49.83	49.74	0.40
155	0.23839	608.19	608.50	0.37008	13.92	46.28	46.27	0.39
156	0.24211	608.44	607.77	0.36979	14.14	46.31	46.30	0.38
157	0.25529	608.02	608.41	0.36993	14.68	47.02	47.04	0.37
158	0.24243	607.91	608.09	0.36966	13.85	47.36	47.33	0.40
159	0.25293	607.63	607.92	0.36939	14.69	46.63	46.64	0.37
160	0.24237	607.62	608.01	0.36944	14.04	46.73	46.70	0.39
161	0.26178	609.05	610.84	0.37203	13.84	50.85	50.88	0.43
162	0.25479	609.93	608.64	0.37123	14.39	47.70	47.74	0.39
163	0.23558	608.15	609.95	0.37094	13.60	46.69	46.71	0.40

Board ID	Mass (kg)	Length (mm)	Width (mm)	Area (m^2)	Thickness (mm)	Bulk density ($kg \cdot m^{-3}$)	Bulk density from Eq.4 ($kg \cdot m^{-3}$)	Bulk density standard uncertainty ($kg \cdot m^{-3}$)
164	0.24729	608.08	609.44	0.37059	14.57	45.81	45.86	0.37
165	0.23367	607.89	609.39	0.37044	13.82	45.66	45.68	0.38
166	0.23657	607.48	607.85	0.36926	14.05	45.59	45.57	0.38
167	0.24508	607.45	607.85	0.36924	14.53	45.67	45.67	0.37
168	0.23754	607.50	607.77	0.36922	14.07	45.72	45.70	0.38
169	0.24482	607.46	608.00	0.36934	14.48	45.78	45.78	0.37
170	0.23931	607.50	608.02	0.36937	14.12	45.88	45.87	0.38
171	0.24648	607.53	608.13	0.36946	14.51	45.99	45.99	0.37
172	0.24030	607.59	607.95	0.36938	14.12	46.09	46.08	0.38
173	0.24836	607.59	608.16	0.36951	14.56	46.16	46.17	0.37
174	0.23857	607.60	608.12	0.36949	13.94	46.31	46.30	0.36
175	0.24900	607.64	608.04	0.36947	14.56	46.28	46.29	0.37
176	0.24047	608.11	608.26	0.36989	14.12	46.04	46.04	0.38
177	0.24577	608.11	608.34	0.36994	14.41	46.11	46.13	0.37
178	0.24202	607.54	609.27	0.37016	13.78	47.47	47.46	0.40
179	0.25743	607.53	609.31	0.37017	14.79	47.03	47.07	0.37
180	0.24039	607.56	607.61	0.36916	13.77	47.31	47.25	0.40
181	0.25808	607.58	609.00	0.37002	14.88	46.87	46.90	0.37
182	0.23516	607.58	609.20	0.37014	13.56	46.86	46.84	0.40
183	0.25608	607.60	609.43	0.37029	14.90	46.43	46.48	0.37
184	0.23908	607.59	609.45	0.37030	13.92	46.37	46.38	0.39
185	0.25334	607.55	609.31	0.37019	14.84	46.11	46.16	0.36
186	0.27082	608.16	609.12	0.37044	14.88	49.12	49.15	0.38
187	0.25098	608.13	609.22	0.37048	13.78	49.17	49.15	0.41
188	0.27018	608.01	609.34	0.37048	14.96	48.76	48.79	0.38
189	0.24911	607.99	609.47	0.37055	13.78	48.79	48.78	0.41
190	0.26908	608.08	609.17	0.37042	15.02	48.35	48.39	0.37
191	0.22959	607.74	607.96	0.36948	14.09	44.09	44.10	0.36
192	0.23212	607.76	607.83	0.36941	13.64	46.08	46.04	0.39
193	0.24449	608.12	609.15	0.37044	14.98	44.05	44.12	0.34
194	0.26476	607.62	609.10	0.37010	13.66	52.36	52.29	0.44
195	0.24164	607.58	609.01	0.37002	15.01	43.52	43.59	0.34
196	0.26288	607.55	609.32	0.37019	13.92	51.03	50.99	0.42
197	0.23781	607.47	609.03	0.36997	14.73	43.65	43.71	0.34
198	0.24999	607.49	609.02	0.36997	13.76	49.11	49.07	0.42
199	0.23412	607.55	609.11	0.37007	14.86	42.57	42.58	0.31
200	0.25074	607.54	609.02	0.37000	13.65	49.67	49.62	0.42
201	0.26582	610.29	608.62	0.37143	13.67	52.36	52.33	0.45

Board ID	Mass (kg)	Length (mm)	Width (mm)	Area (m^2)	Thickness (mm)	Bulk density ($kg{\cdot}m^{-3}$)	Bulk density from Eq.4 ($kg{\cdot}m^{-3}$)	Bulk density standard uncertainty ($kg{\cdot}m^{-3}$)
202	0.29201	609.30	608.60	0.37082	15.01	52.45	52.46	0.40
203	0.26923	609.53	608.73	0.37104	13.76	52.74	52.70	0.44
204	0.25787	608.13	609.14	0.37044	13.83	50.35	50.32	0.42
205	0.26442	608.10	609.53	0.37066	13.74	51.94	51.89	0.44
206	0.28500	608.13	609.49	0.37065	14.90	51.61	51.62	0.40
207	0.26102	608.27	609.33	0.37064	13.62	51.70	51.65	0.44
208	0.25893	607.82	609.28	0.37033	13.77	50.77	50.73	0.43
209	0.23276	607.56	607.33	0.36899	14.11	44.72	44.70	0.37
210	0.23880	607.62	607.35	0.36904	14.45	44.79	44.79	0.36
211	0.23379	607.66	607.38	0.36908	14.13	44.83	44.81	0.37
212	0.24110	607.35	607.78	0.36914	14.50	45.04	45.04	0.36
213	0.23229	607.35	607.95	0.36924	13.92	45.19	45.17	0.38
214	0.24128	607.77	607.39	0.36915	14.47	45.16	45.16	0.36
215	0.23430	607.36	608.04	0.36930	14.00	45.31	45.29	0.38
216	0.24369	607.72	607.45	0.36916	14.57	45.30	45.30	0.36
217	0.23417	607.70	607.47	0.36916	13.95	45.46	45.44	0.38
218	0.24502	607.74	607.45	0.36917	14.62	45.41	45.41	0.36
219	0.23597	607.68	607.48	0.36915	14.00	45.67	45.64	0.38
220	0.24628	607.84	607.39	0.36920	14.58	45.74	45.74	0.36
221	0.24341	608.40	608.06	0.36994	13.99	47.04	47.03	0.39
222	0.25056	607.89	607.95	0.36957	14.75	45.97	45.99	0.36
223	0.23291	607.42	607.71	0.36914	13.87	45.48	45.45	0.38
224	0.23884	607.79	609.05	0.37018	13.88	46.48	46.48	0.36
225	0.25541	607.76	609.04	0.37015	14.87	46.42	46.46	0.36
226	0.24070	607.83	609.12	0.37024	13.89	46.82	46.82	0.39
227	0.25889	607.97	609.08	0.37030	14.93	46.82	46.86	0.37
228	0.23702	607.92	609.39	0.37046	13.54	47.26	47.25	0.41
229	0.26093	607.92	609.16	0.37032	14.95	47.13	47.17	0.37
230	0.24258	607.85	609.03	0.37020	13.76	47.64	47.63	0.40
231	0.22768	607.37	608.19	0.36940	14.13	43.61	43.62	0.36
232	0.22694	607.45	608.06	0.36937	14.19	43.31	43.33	0.36
233	0.22479	607.27	608.00	0.36922	14.15	43.02	43.03	0.36
234	0.22489	607.27	607.75	0.36907	14.22	42.84	42.85	0.35
235	0.22581	607.24	607.79	0.36907	14.31	42.76	42.77	0.35
236	0.24054	607.66	608.02	0.36947	14.03	46.42	46.40	0.39
237	0.25111	607.62	608.02	0.36945	14.64	46.44	46.44	0.37
238	0.23956	607.61	608.14	0.36951	13.92	46.57	46.55	0.39
239	0.24402	607.46	609.38	0.37017	14.67	44.95	45.00	0.36

Board ID	Mass (kg)	Length (mm)	Width (mm)	Area (m^2)	Thickness (mm)	Bulk density (kg·m^{-3})	Bulk density from Eq.4 (kg·m^{-3})	Bulk density standard uncertainty (kg·m^{-3})
240	0.25009	607.78	608.18	0.36964	14.78	45.79	45.82	0.36
241	0.23791	607.72	607.87	0.36941	14.46	44.53	44.55	0.36
242	0.23304	607.74	608.21	0.36963	14.09	44.75	44.75	0.37
243	0.26106	607.91	609.27	0.37038	14.81	47.61	47.65	0.38
244	0.24468	607.93	609.02	0.37024	13.76	48.03	48.01	0.40
245	0.26690	609.12	607.99	0.37034	15.01	48.03	48.06	0.37
246	0.23520	607.68	608.45	0.36974	13.80	46.10	46.09	0.39
247	0.24026	607.65	608.36	0.36967	14.46	44.95	44.97	0.36
248	0.23200	607.60	608.19	0.36954	14.14	44.42	44.43	0.37
249	0.23186	607.49	608.23	0.36950	14.23	44.10	44.10	0.33
250	0.22913	607.51	607.91	0.36931	14.13	43.91	43.91	0.36
251	0.25390	607.79	608.36	0.36976	14.35	47.86	47.85	0.39
252	0.23053	607.18	607.84	0.36907	14.51	43.04	43.06	0.35
253	0.22476	607.20	607.83	0.36907	14.11	43.15	43.15	0.36
254	0.22826	607.73	607.25	0.36904	14.34	43.14	43.15	0.35
255	0.22571	607.67	607.23	0.36900	14.13	43.28	43.28	0.36
256	0.23038	607.63	607.25	0.36898	14.43	43.28	43.29	0.35
257	0.22798	607.83	607.28	0.36912	14.24	43.36	43.37	0.36
258	0.23472	607.84	608.97	0.37016	13.74	46.16	46.16	0.39
259	0.25173	607.84	608.94	0.37014	14.75	46.12	46.15	0.36
260	0.22631	607.47	607.28	0.36890	13.94	44.02	43.99	0.37
261	0.23794	607.52	607.28	0.36893	14.67	43.96	43.97	0.35
262	0.22622	607.57	607.30	0.36898	13.86	44.24	44.21	0.37
263	0.23858	607.27	607.76	0.36907	14.66	44.11	44.13	0.35
264	0.22992	607.28	607.81	0.36911	14.05	44.34	44.33	0.37
265	0.23724	607.67	607.40	0.36910	14.48	44.38	44.39	0.36
266	0.23140	607.28	607.69	0.36904	14.09	44.50	44.49	0.37
267	0.23739	607.23	607.79	0.36907	14.43	44.57	44.57	0.36
268	0.23064	607.42	607.99	0.36931	14.25	43.84	43.85	0.36
269	0.23042	607.36	607.75	0.36912	14.28	43.73	43.74	0.36
270	0.23390	607.36	607.76	0.36913	14.44	43.88	43.89	0.35
271	0.22713	607.40	608.07	0.36934	14.02	43.88	43.88	0.36
272	0.23571	607.38	607.84	0.36919	14.53	43.93	43.95	0.35
273	0.22633	607.32	608.08	0.36930	13.92	44.03	44.02	0.37
274	0.23778	607.37	607.92	0.36923	14.60	44.10	44.11	0.32
275	0.23003	607.40	607.98	0.36929	14.08	44.26	44.25	0.37
276	0.23244	607.19	607.74	0.36901	14.46	43.56	43.58	0.35
277	0.22216	607.18	607.60	0.36892	13.80	43.63	43.61	0.37

Board ID	Mass (kg)	Length (mm)	Width (mm)	Area (m^2)	Thickness (mm)	Bulk density ($kg·m^{-3}$)	Bulk density from Eq.4 ($kg·m^{-3}$)	Bulk density standard uncertainty ($kg·m^{-3}$)
278	0.23439	607.26	607.58	0.36896	14.57	43.62	43.63	0.35
279	0.22569	607.25	607.64	0.36899	13.98	43.77	43.76	0.36
280	0.23359	607.25	607.58	0.36895	14.44	43.86	43.86	0.35
281	0.23869	608.05	607.57	0.36943	14.09	45.85	45.83	0.38
282	0.24614	607.49	608.06	0.36939	14.54	45.84	45.85	0.37
283	0.24003	607.55	607.89	0.36932	14.14	45.96	45.94	0.38
284	0.23118	607.39	607.76	0.36915	14.13	44.34	44.33	0.37
285	0.23798	607.45	607.93	0.36929	14.54	44.33	44.35	0.35
286	0.23502	607.46	608.05	0.36937	14.29	44.52	44.53	0.36
287	0.23932	607.44	608.08	0.36937	14.54	44.57	44.58	0.35
288	0.22727	607.43	608.11	0.36938	13.76	44.71	44.69	0.36
289	0.24233	607.41	607.86	0.36922	14.66	44.77	44.79	0.35
290	0.23232	607.47	607.78	0.36921	13.98	45.01	45.00	0.36
291	0.25676	608.69	609.11	0.37076	14.06	49.26	49.26	0.39
292	0.24629	607.64	608.10	0.36951	14.49	45.99	46.00	0.37
293	0.23782	608.09	607.58	0.36946	13.94	46.18	46.15	0.39
294	0.25030	608.18	607.60	0.36953	14.71	46.05	46.06	0.37
295	0.24169	608.19	607.69	0.36959	14.13	46.28	46.27	0.38
296	0.24907	607.97	608.17	0.36975	14.00	48.11	48.09	0.40
297	0.25996	608.07	608.30	0.36989	14.61	48.11	48.12	0.38
298	0.24608	608.21	608.37	0.37002	13.87	47.95	47.93	0.4
299	0.24173	607.39	607.85	0.36920	14.53	45.07	45.07	0.33
300	0.23294	607.41	607.97	0.36929	13.96	45.18	45.16	0.38
301	0.24616	607.44	608.01	0.36933	14.70	45.35	45.36	0.36

5.4.2. Rejected Boards

78 boards (26 %) among 300 showed surface imperfections such as grooves across the board surfaces. 5 locations of the groove areas of ID 199 board were representatively examined using a stylus type surface profilometer (Dektak XT, Bruker). These measurements were performed independent of the surface roughness measurements of Table 2. The height differences from the peaks to the valleys in the grooves were distributed from ≈ 216 µm to ≈ 325 µm. The distances from the peaks to the adjacent peaks were distributed from ≈ 1.8 mm to ≈ 2.5 mm. The height differences from the mean levels (i.e., roughness average, R_a) in the groove approximated by using the relation (= peak height – (peak height + valley height) / 2) were distributed from ≈ 58 µm to ≈ 163 µm. The approximated R_a values of the groove were about 2- to 7- fold higher than the R_a (24.2 µm) of the pristine board sample. Due to potential parasitic

heat flow through the groove for the guarded-hot-plate test, 78 boards were excluded from the material lot (222 boards were accepted), and listed below:

042, 046, 066, 067, 078, 082, 089, 092, 093, 095, 101, 111, 134, 135, 136, 137, 139, 146, 147, 154, 156, 166, 167, 168, 169, 170, 171, 172, 173, 174, 175, 178, 179, 180, 181, 182, 183, 194, 195, 196, 197, 198, 199, 200, 223, 227, 228, 236, 237, 238, 239, 243, 246, 247, 248, 249, 250, 251, 268, 269, 270, 271, 272, 273, 274, 275, 284, 285, 286, 287, 288, 289, 290, 296, 298, 299, 300, 301

5.5. Bulk Density Metrological Traceability

Table 4 summarizes the calibration information for the electric balance, gage blocks, and surface plate used to perform the bulk density measurements. The calibration uncertainties are included in Appendix 1.1. Internal checks (Items 2, 5, and 6) were conducted by the operators during the measurement process.

Table 4. Calibration information for the bulk density measurements.

Item	Equipment Calibrated	Description of standard	Calibration		
			Organization	Date	Cert. Number
1	Mettler balance SG32001DL	Weight set 632 traceable to NIST	Mettler Toledo	2023	072908-046-032823
2	Mettler balance check	100 g, 200 g, 300 g masses	732.03		-
3	14.3 mm gage block	Standards of the United States	NIST	2022	685-O-0000038571-22
4	12 in. gage blocks L4M041 & L4M042	Standards of the United States	NIST	2023	685-O-0000038571-22
5	Mitutoyo 0 to 300 mm height gage 192-670-10	Nominal 14.3 mm gage block	732.03		-
6	Mitutoyo 0 to 600 mm height gage 192-672-10	24 in. gage block	732.03		-
7	Starrett surface plate	Traceable to NIST	Laboratory Testing	2022	NIS001-22-04-01845-1
8	Troemner E/B weight set 4000010240	Reference masses traceable to NIST (684/289871-17)	Troemner	2022	220577411-2

6. Thermal Conductivity Measurements

This section describes the experimental design, specimens, guarded-hot-plate (GHP) measurements, and determinations of thermal conductivity.

6.1. Experimental Design

For the measurement of thermal conductivity, a split-plot designed experiment was planned and carried out, with board density being the whole-plot or hard-to-change factor and temperature being the split-plot factor. The terminology whole-plot and split-plot reference the origin of this type of experiment design, agricultural experiments, where one factor is applied to an entire field, i.e. the whole-plot, and another factor is applied to a part of a field, i.e. split-plot. In this case, density is "applied" to a pair of boards, and a temperature is applied to a measurement of a pair of boards. A pair of boards plays the role of the whole-plot, so density plays the role of the whole-plot factor. A single measurement plays the role of the split-plot, so temperature plays the role of the split-plot factor.

Three levels of density and five levels of temperature were used, allowing to fit a linear trend in bulk density and a cubic trend in temperature. The temperatures were set according to past practice and industry demands; the levels of density were selected appropriately from the population of boards, 43.6 $kg \cdot m^{-3}$ for the low bulk density, 48.1 $kg \cdot m^{-3}$ for the mid bulk density, and 52.0 $kg \cdot m^{-3}$ for the high bulk density. Since the GHP apparatus requires board pairs, the previous bulk densities are pair averages.

This design increased experimental efficiency over a completely randomized design, requiring fewer total boards and less changing of boards in and out of the GHP apparatus. That is because for a completely randomized design, no pair of boards would be measured twice. Five pairs of boards with approximately the same average density, would be required to make measurements for five different temperatures. For the same number of measurements, with three density levels, that is fifteen pairs of boards instead of three pairs.

6.1.1. Model Input Quantities - Bulk Density and Temperature

Table 5 ranks the specimens by input temperature (T_m) and by bulk density (ρ_b) within each temperature setting. Each specimen pair was tested at five levels of temperature. The first column assigns a test sequence for the guarded-hot-plate measurements. The test sequence outlined in Table 5 involved a total of 20 (=3×5+5).

Table 5. Test sequence and settings for the 3 pairs of test specimens

Test sequence	Specimen pair	Specimen ID	Bulk density ($kg \cdot m^{-3}$)	T_m (K)
1	1	277 278	43.61 43.63	282
2				290
3				298
4				306
5				314
6	2	297 054	48.12 48.11	282
7				290
8				298
9				306
10				314
11	3	144 115	51.96 52.05	282
12				290
13				298
14				306
15				314
16	2	297 054	48.12 48.11	282
17				290
18				298
19				306
20				314

6.1.2. Guarded-Hot-Plate Method

Figure 5 illustrates the main components of a guarded-hot-plate apparatus designed for operation near ambient temperature conditions. The apparatus is cylindrically symmetric about the axis indicated in Fig. 5. The plates are horizontal, and heat flow (Q) is vertical (up/down) through the pair of specimens. The specimens with nearly the same density, size and thickness are placed on each surface of the guarded hot plate and clamped by the cold plates. The guarded hot plate and the cold plates provide constant-temperature boundary conditions to the specimen surfaces. With proper guarding, lateral heat flows (Q_{gap} and Q_{edge}) are reduced to negligible proportions. Under steady-state conditions, the apparatus provides one-dimensional heat flow (Q) normal to the meter area of the specimen pair. A secondary guard is provided by an enclosed chamber that conditions the ambient air surrounding the plates to a temperature near to the mean specimen temperature (i.e. average surface temperatures of the hot and cold plates in contact with the specimens). The thermal transmission calculations, based on heat flux measurements from the guarded-hot-plate apparatus, can be expressed in Eq.5.

$$\lambda_{exp} = \frac{QL_{ave}}{2A\Delta T_{ave}} \qquad (5)$$

where

L_{ave} = the mean values of the two specimen thicknesses;
ΔT_{ave} = the mean temperature difference;
$2A$ = the metered area that heat flows through.

Values of λ_{exp} are reported at the mean specimen temperature, T_m, given by Eq. (6).

$$T_m = \frac{T_h + T_c}{2} = \frac{T_h + (T_{c1} + T_{c2})/2}{2} \qquad (6)$$

The thermal transmission properties of insulation materials determined from standard test methods typically include multiple mechanisms of heat transfer such as conduction, radiation, and possibly convection. Therefore, the adjective "apparent" when describing the thermal conductivity of insulation materials is sometime used. The term thermal conductivity is defined to mean apparent thermal conductivity in this report.

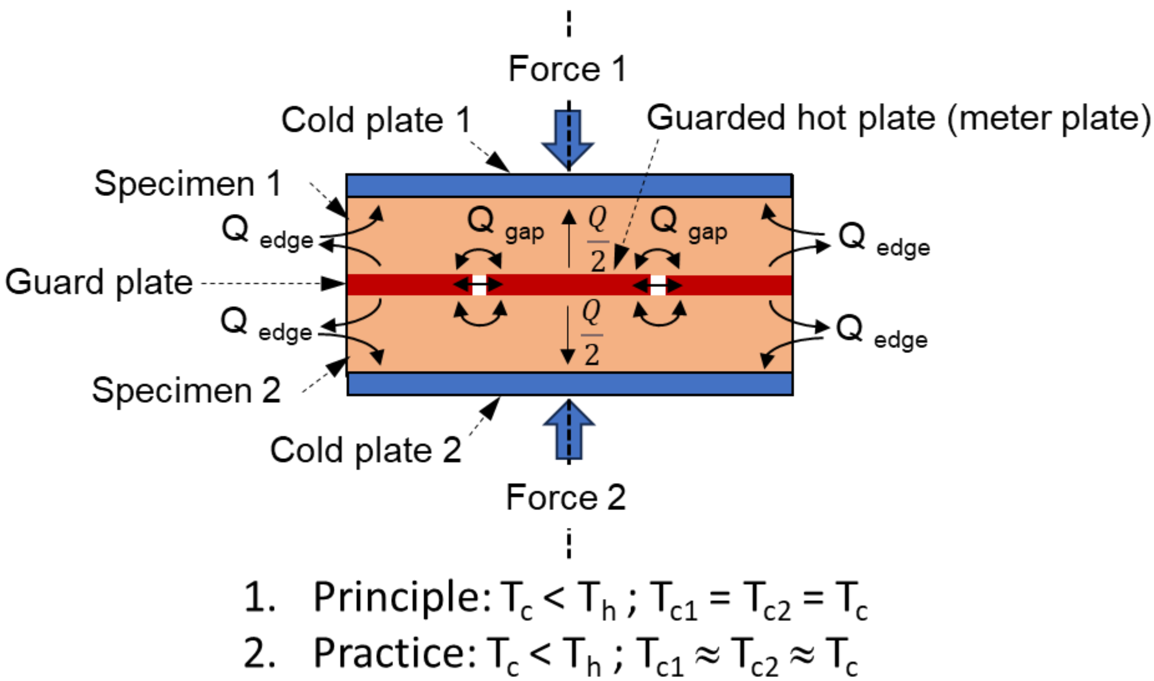

Fig. 5. Guarded-hot-plate schematic, double-sided mode of operation – vertical heat flow

6.1.3. 1016 mm Guarded-Hot-Plate Apparatus

The NIST 1016 mm guarded-hot-plate apparatus and uncertainty assessment, under near ambient conditions, have been described previously [12]. The apparatus plates, 1016 mm in diameter, were fabricated using 6016-T6 aluminum alloy and the surfaces in contact with the specimens were anodized black to have an emittance of 0.89. The meter plate is nominally 406 mm in diameter and is physically separated from the surrounding guard plate by an air gap as shown in Fig. 5.

6.1.4. Test procedure

The guarded-hot-plate measurements for production of SRM 1453a started on February 12, 2024 and concluded on April 16, 2024. The thermal conductivity measurement of each pair of foam specimens was completed in one to two days. During the production tests, the EPS board specimens (610 mm by 610 mm) were installed in the guarded-hot-plate apparatus and encircled with the fibrous polyester blanket insulation. This polyester insulation material was selected because of its compressibility and similar thermal conductivity. In separate guarded-hot-plate tests, the thermal conductivities of 12.7 mm thick specimens of polyester blanket specimens were determined to be 0.037 $W{\cdot}m^{-1}{\cdot}K^{-1}$, 0.041 $W{\cdot}m^{-1}{\cdot}K^{-1}$, 0.045 $W{\cdot}m^{-1}{\cdot}K^{-1}$ at T_m of 282 K, 298 K, 314 K, respectively. During the steady-state test period, data for Q, T_h and T_c were collected every 2 min. When the plate temperatures were within 0.05 K of their target temperatures and Q no longer changed monotonically, data were collected for 4 h and averaged over that time interval.

6.2. Data summary

Table 6 summarizes the main experimental results – specimen information, input estimates, and the output estimate for measured thermal conductivity (λ_{exp}) – for the 3 specimen pairs specified in Table 5. The rows of data in Table 6 are grouped by T_m from 282 K to 314 K and, within each level of T_m, the average specimen densities (ρ_s) are arranged from lowest to highest value. The columns of data are grouped into four major sections: 1) specimen material property, 2) input quantities for Eq. (14), 3) secondary quantities, and 4) resultant thermal conductivity (λ). The notation "1" and "2" in Table 6 designate the top and bottom specimen, respectively, as illustrated in Fig. 6. The bulk density parameter is the average of the bulk densities listed in Table 5 and $\rho_{in\text{-}situ}$ is the average of the densities of the specimen pair obtained using the in-situ test thickness under the guarded-hot-plate tests. During testing, the specimens were compressed slightly under load, thereby decreasing the in-situ specimen thickness (L_{ave}) and increasing the bulk density. The *in situ* average bulk density was determined by multiplying the average bulk density by the ratio of the average thickness to the *in situ* average thickness (L_{ave}). No adjustments were made for changes in the specimen lateral surface area or mass for calculating $\rho_{in\text{-}situ}$. The differences between the average bulk densities and *in situ* average bulk densities were 1.0 % or less. The input temperature estimates, T_h, T_{c1}, and T_{c2} were within 0.01 K, or less, of their respective set-point temperatures. The estimates of $Q/2$ ranged from 6.3 W to 7.0 W for T_m from 282 K to 314 K. Estimates for A were corrected for thermal expansion effects of the meter-plate radius.

Table 6. SRM 1453a thermal conductivity data

T_m (K)	ρ_s (Kg·m^{-3})	$\rho_{in\text{-}situ}$	T_h (K)	T_{c1} (K)	T_{c2} (K)	Q/2 (W)	A (m^2)	L_{ave} (mm)	T_a (K)	P_a (kPa)	RH (%)	F (Pa)	λ_{exp} (W·m^{-1}·K^{-1})
282	43.6	44.1	293.00	271.00	271.00	6.368	0.12981	14.04	282.00	100.6	19	244	0.03130
282	48.1	48.3	293.00	271.00	271.01	6.323	0.12981	14.19	282.00	100.7	21	239	0.03142
282	52.0	52.2	293.00	271.00	271.00	6.342	0.12981	14.23	282.00	99.5	19	210	0.03160
282	48.1	48.4	293.00	271.00	271.00	6.337	0.12981	14.18	282.00	99.8	26	217	0.03147
290	43.6	44.0	301.00	279.00	279.00	6.532	0.12986	14.07	290.00	101.4	9	236	0.03217
290	48.1	48.3	301.00	279.00	279.00	6.487	0.12986	14.20	290.00	99.1	10	239	0.03225
290	52.0	52.2	301.00	279.00	279.00	6.506	0.12986	14.25	290.00	99.8	10	228	0.03245
290	48.1	48.3	301.00	279.00	278.99	6.497	0.12986	14.21	290.00	100.2	8	241	0.03231
298	43.6	43.9	309.00	287.00	287.00	6.690	0.12991	14.11	298.00	101.1	5	239	0.03302
298	48.1	48.2	309.00	287.00	287.00	6.639	0.12991	14.23	298.00	100.9	5	245	0.03306
298	52.0	52.0	309.00	287.00	287.00	6.654	0.12991	14.30	298.00	99.6	4	214	0.03329
298	48.1	48.1	309.00	287.00	287.00	6.641	0.12991	14.25	298.00	99.9	4	231	0.03311
306	43.6	43.8	317.00	295.00	295.00	6.843	0.12996	14.14	306.00	99.6	5	246	0.03383
306	48.1	48.1	317.00	295.00	295.00	6.798	0.12996	14.25	306.00	100.6	5	231	0.03387
306	52.0	51.9	317.00	295.00	295.00	6.805	0.12996	14.31	306.00	99.0	6	211	0.03407
306	48.1	48.1	317.00	294.99	294.99	6.799	0.12996	14.26	306.00	99.2	6	240	0.03390
314	43.6	43.7	325.00	303.00	303.00	7.003	0.13001	14.16	314.00	98.7	5	246	0.03466
314	48.1	48.1	325.00	303.00	303.00	6.955	0.13001	14.26	314.00	100.3	7	232	0.03467
314	52.0	51.9	325.00	303.00	303.00	6.956	0.13001	14.33	314.00	97.8	7	239	0.03486
314	48.1	48.1	325.00	303.00	303.00	6.955	0.13001	14.28	314.00	100.6	6	236	0.03471

During any given test, the secondary factors (T_a, P_a, *RH, and F*) were either controlled or recorded. The chamber air temperature (T_a) was controlled to be the same temperature as T_m (within 0.1 K, or less). The chamber air pressure (P_a) with the site barometric conditions, which varied from 97.8 kPa to 101.4 kPa. The chamber *RH* varied inversely with chamber dry-bulb air temperature (T_a). The clamping pressure (*F*) was determined by averaging the loading force applied by each cold plate divided by the surface area of the cold plate, which was corrected for thermal expansion effects. The maximum clamping pressure of 246 Pa (0.246 kPa) in Table 6 was about 3 orders of magnitude lower than the compression yield point of the polystyrene panel stated in Appendix 3.

Table 7. Summary statistics for fixed input quantities and secondary quantities

	ΔT (K)	L_{ave} (mm)	P_a (kPa)	F (Pa)
Mean	22.000	14.21	99.9	233.2
Std. Dev.	0.003	0.08	0.9	11.5

7. Analysis and Uncertainty Evaluation

Section 7 presents statistical analyses of the thermal conductivity data for the SRM 1453a production test, the development of the certified equation, assessment of uncertainty, and information on metrological traceability.

7.1. Data Evaluation

Figures 6 and 7 plot the values of λ_{exp} from Table 7 as a function of the input variables ρ_s and T_m, respectively. For Fig. 6, the three levels of ρ from 43.6 kg·m^{-3} to 52.0 kg·m^{-3} and five levels of T_m from 282 K to 314 K are given for each graph.

A cursory review of the two plots suggests that λ_{exp} is slightly sensitive to ρ, which is supported by the linear least square fits in Figure 6. For the bulk density range of 43.6 kg·m^{-3} to 52.0 kg·m^{-3}, the change in thermal conductivity with respect to bulk density was relatively small compared to that of Fig. 7 and, apparently, increased as bulk density increased. Figure 7 shows that the dependency of λ_{exp} on T_m is nearly linear in the range of T_m applied for the current SRM.

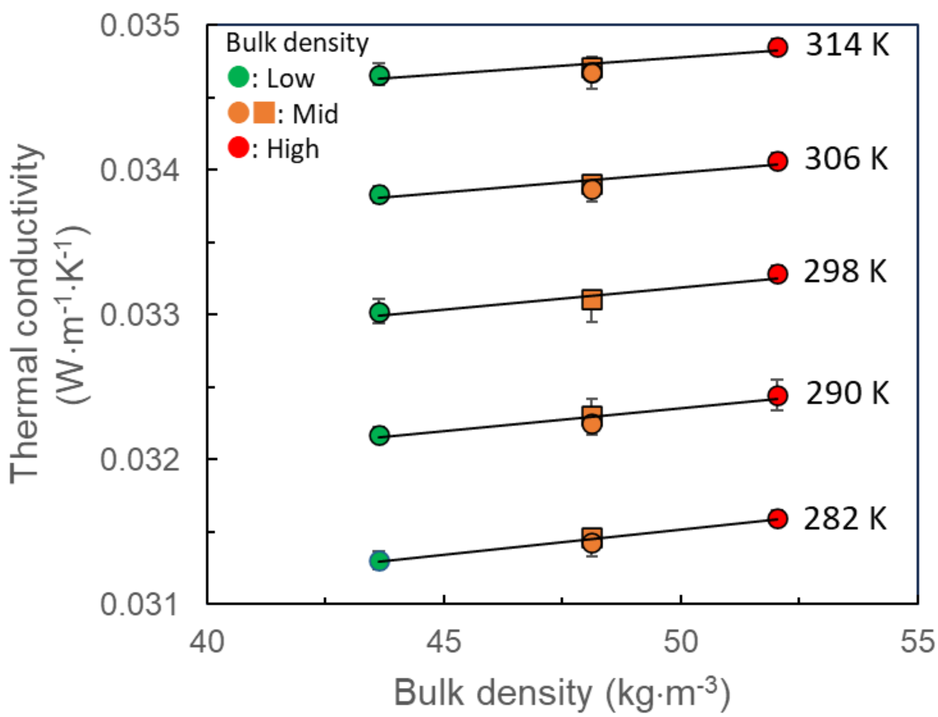

Fig. 6. Scatter plot of λ_{exp} versus ρ_s at several temperatures.

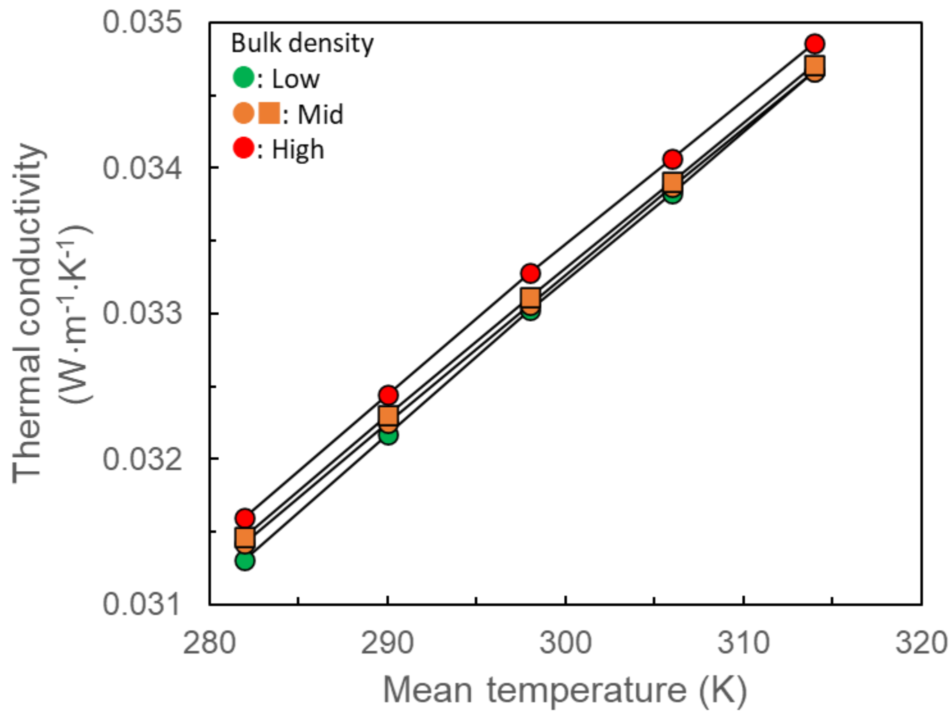

Fig. 7. Scatter plot of λ_{exp} versus T_m for several bulk densities.

7.2. Bulk density of the metered section versus entire sample

The data in Fig.6 indicate that λ_{exp} is slightly dependent on ρ. To determine the effect of the metered section density, the insulation specimens located in the upper and lower region of the meter plate were cut to create 406 mm cylindrical samples using a jig saw. The metered section bulk density is defined in Eq. (7).

$$\rho_m = \frac{m_m}{(\pi r^2)\times L_m} \qquad (7)$$

where the subscript m refers to the metered section, and r is the radius of the round cylinder. To preserve particular specimens for future measurements, a specific subset of only four specimens (two pairs) was selected for cutting. m_m was measured by a digital weighing balance with 0.0001 kg resolution. After placing the cylindrical sample on a granite surface plate, r was determined by averaging three length measurements using a steel ruler with 0.05 cm resolution. L_m was averaged from four height gage measurements (0.01 mm resolution).

Table 8 shows the specimen density (ρ_s) and meter section density (ρ_m), and the difference (ρ_m-ρ_s) of the densities. The differences range from -0.9 kg·m^{-3} to 1.2 kg·m^{-3}, and show no clear trends. The mean and standard deviation of the differences are 0.23 kg·m^{-3} and 0.88 kg·m^{-3}, respectively. A 95 % Student's t interval for the mean density difference includes zero. Therefore, there does not exist strong evidence that the mean difference in densities for the meter section and entire specimen is nonzero. This supports not correcting the bulk density of the sample measured on the surface plate.

Table 8. Comparison of specimen and meter area bulk densities

ID	Density level	ρ_s (kg·m^{-3})	ρ_m (kg·m^{-3})	(ρ_m-ρ_s) (kg·m^{-3})
277	Low	43.63	42.42	1.21
278	Low	43.62	43.10	0.52
144	High	52.02	51.91	0.11
115	High	52.04	52.94	-0.90
				(Mean) 0.23
				(Std. dev.) 0.88

Practically, it is difficult to know how often the sample geometry of the 406 mm circle is used for the thermal tests. Within current knowledge, typical sample geometries of commercial heat flow meter and guarded hot plate are square shapes. Moreover, the procedures of the measurements described in Section 5 provide all physical properties with metrological traceabilities for bulk density. Based on these reasons, the bulk density data listed in Table 2 of Section 5 are used for the certified equation of SRM 1453a relating thermal conductivity to mean temperature and bulk density.

7.3. Development of the certified equation and uncertainty quantification

The λ_{exp} from Table 6 are modeled using a mixed effects statistical model. Since each panel pair is measured at each T_m, the model yields separate cubic polynomials relating λ_{exp} to T_m for each panel pair. Besides the three distinct cubic polynomials, one for each panel pair, the model also yields an average cubic polynomial relating λ_{exp} to T_m, which is the cubic polynomial in T_m reported in the certified equation.

Besides cubic polynomials relating λ_{exp} to T_m for each panel pair, the model also yields a linear relationship relating λ_{exp} to ρ_s. Since ρ_s is fixed for each panel pair, it is only possible to estimate a single linear trend, which is the linear relationship in ρ_s reported in the certified equation.

Statistical inference (estimation of the model parameters) is performed from the Bayesian perspective, so prior distributions must be selected. Normal distributions for parameters defined on $\mathbb{R}$ or half-normal distributions for parameters defined on $\mathbb{R}_+$ are used. The parameters of those normal prior distributions are selected to be only weakly informative, restricting only implausibly large values for the polynomial coefficients and parameters quantifying the variability in the observed measurements of λ_{exp}.

The estimated relative expanded uncertainty for the certified equation is 1.9 %. To understand the interpretation of this expanded uncertainty, consider the following thought experiment. Imagine sampling randomly a new pair of boards with average bulk density $\rho_{s,\,\text{new}}$ and measured at the mean temperature $T_{m,\,\text{new}}$. The mixed effects model can be used to predict the thermal conductivity λ_{new} for that bulk density, mean temperature combination; however, the model can be used many times to predict many different values of λ_{new} because there could be many different panel pairs with the same average bulk density but that behave slightly differently as a function of average temperature. Further, each prediction realizes a different experimental error, and the coefficients defining the linear relationship between thermal conductivity and bulk density and the coefficients defining the average cubic polynomial between thermal conductivity and average temperature are only estimated, not known exactly. By making a histogram of the many random predictions of λ_{new} a 95 % prediction interval for λ_{new} may be calculated by finding the middle 95 % of the histogram. The procedure described in this thought experiment can be carried out for many combinations of $\rho_{s,\,\text{new}}$ and $T_{m,\,\text{new}}$ over the range of valid values specified for this SRM. Taking the half-widths of all of those 95 % prediction intervals, and then taking the maximum of all the half-widths yields the 1.9 % relative expanded uncertainty.

Note that the relative expanded uncertainty of 1.9 % is only relevant to using the certified equation to predict the thermal conductivity of a board pair measured on the GHP apparatus. It is not comparable to the uncertainty evaluation for individual measurements of thermal conductivity considered in Appendix 2.

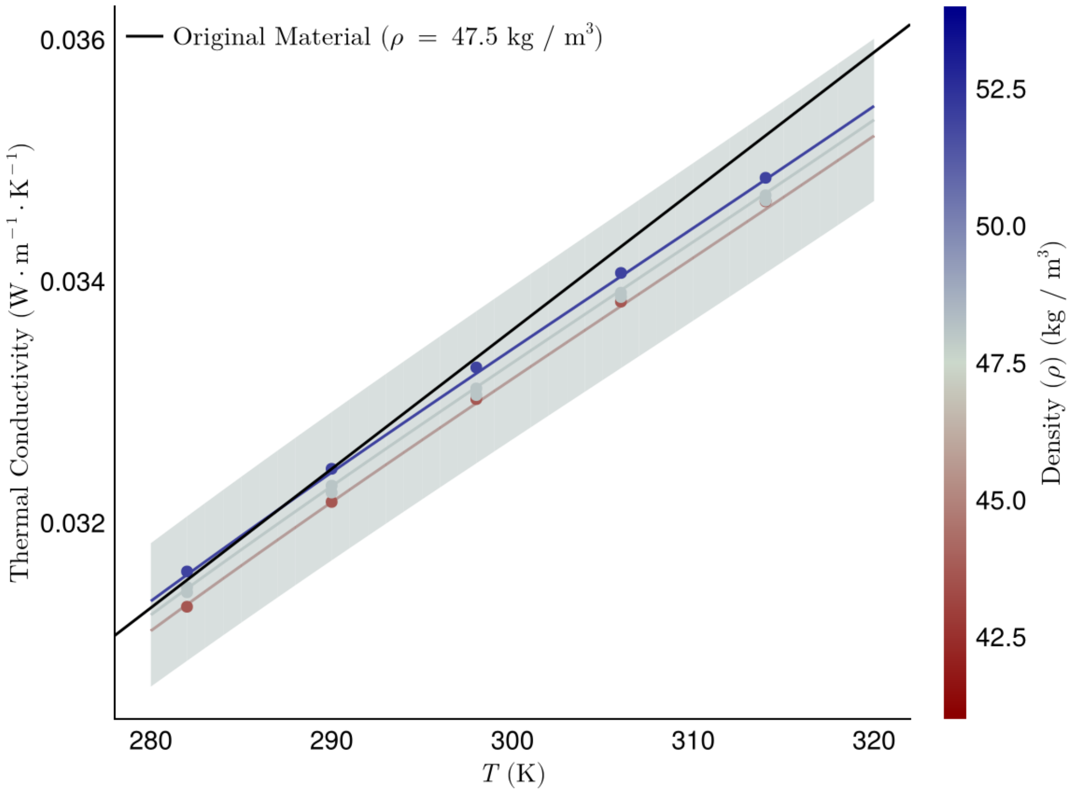

Fig. 8. Scatter plot of λ_{exp} versus T_m (points), depictions of the certified equation (red, gray, and blue lines), ±1.9 % coverage bands for the certified equation for a density of approximately 47.5 kg (gray band), and the certified equation for the original 1453 material (black line).

Figure 8 again plots the values of λ_{exp} versus T_m from Table 6, just as in Fig. 7. However, Fig. 8 adds depictions of the certified equation for three distinct values of bulk density, the corresponding ±1.9 % coverage bands, as well as the certified equation for the original material 1453 material for comparison. Clearly from Fig. 8, the observed variability in the λ_{exp} is suitably enveloped by the 1.9 % relative expanded uncertainty. Also, from Fig. 8, we see that the certified equation for 1453 material is similar to the new equation, but not exactly the same. Thermal conductivity appears to increase more quickly with temperature for the original 1453 material; although, the difference is not statistically significant over the range of temperatures considered.

7.4. Thermal Conductivity Metrological Traceability

Table 9 summarizes the calibration information for the guarded-hot-plate equipment. The uncertainties due to calibration of the artifacts and equipment were included in the extended uncertainty analysis described in Appendix 2.

Table 9. Calibration information for the thermal conductivity measurements

Item	Equipment Calibrated	Organization	Date	Cert. Number
1	Digital multimeter S/N: 2919A12149	Keysight Technologies	2023	WO-00364320
2	0.1Ω Standard Resistor S/N: 21736	NIST	2018	684/292309-18
3	Platinum Resistance Thermometer S/N: 290	NIST	2015	685/287694
4	Platinum Resistance Thermometer S/N: 292	NIST	2015	685/287694
5	Platinum Resistance Thermometer S/N: 732	NIST	2015	685/286793
6	Linear position transducers	Internal check		
7	Fused-Quartz Spacers	Internal check		
8	Hot plate diameters	NIST	2015	683/287041-15
9	Load cell S/N: 53722	NIST	2015	684/285454-14
10	Load cell S/N: 53766	NIST	2015	684/285454-14
11	Chamber air pressure S/N: 12323194	Internal check	2023	
12	Chamber relative humidity S/N: 654205	Vaisala	2015	2020433-150818-HMP133YX-654205

8. Certification

Section 8 presents summary information on the properties of interest, values and uncertainty, and instructions for use for Standard Reference Materials 1453a. This information is intended to provide supplementary documentation for the 1453a Certificate.

8.1. Properties of Interest

Standard Reference Material 1453a is an expanded polystyrene foam board certified for thermal conductivity, λ. Each SRM unit as a semi-rigid board consists of a square panel of expanded polystyrene beads. The nominal dimensions of a unit are 608 mm by 609 mm by 14.3 mm (Table 3) and the bulk density ranges from 42 $kg{\cdot}m^{-3}$ to 54 $kg{\cdot}m^{-3}$ (Table 3).

8.2. Values and Uncertainties

Each unit of SRM 1453a is individually certified for bulk density, ρ (the bulk density from Eq.4 in Table 3), and batch certified for thermal conductivity with Eq. (8):

$$\lambda = -0.12383 + 0.001328 \times T_m + 2.9367 \times 10^{-5} \times \rho - 3.9977 \times 10^{-6} \times T_m^2 + 4.3384 \times 10^{-9} \times T_m^3 \quad (8)$$

where λ is the predicted thermal conductivity ($W{\cdot}m^{-1}{\cdot}k^{-1}$), ρ is the bulk density ($kg{\cdot}m^{-3}$), and T_m is the mean specimen temperature (K). Equation (17) is certified to be valid for ρ from 42 $kg{\cdot}m^{-3}$ to 54 $kg{\cdot}m^{-3}$, specimen ΔT of 22 K, and T_m from 282 K to 314 K. The expanded uncertainty for λ values from Eq. (8) is 1.9 % with a coverage factor of $k = 2$.

8.3. Statement of Metrological Traceability

The input quantities for the determination of bulk density and thermal conductivity are metrologically traceable to working references maintained at NIST as described in Sec.5.5 and Sec. 7.4, respectively.

8.4. Instructions for Use

Standard Reference Material 1453a is intended for use as a proven check for the guarded-hot-plate apparatus (or other absolute thermal conductivity apparatus) and for calibration of a heat-flow-meter apparatus over the temperature range of 282 K to 314 K. NIST cannot exclude the use of SRM 1453a for other purposes, but the user is cautioned that other purposes are not sanctioned by the SRM 1453a Certificate.

8.4.1. Storage

For protection and identification, it is recommended that the reference material be stored in the original packaging in a clean, dry environment at temperatures between 15 °C and 30 °C.

8.4.2. Preparation and Conditioning Before Measurement

Prior to the thermal conductivity measurement, the reference material should be conditioned in laboratory conditions of 20 °C to 25 °C and from 40 % RH to 65 % RH until the mass of the unit is stable showing less than 1 % variation within 24 h for two successive measurements. Based on the previous SRM 1453 result, the polystyrene foam is insensitive to changes in humidity.

8.4.3. Thermal Conductivity Measurement

Thermal conductivity measurements should be conducted in accordance with the appropriate ASTM Test Method C 177 [1], C 518 [2], or another similar international standard.

8.4.4. Guidelines and Precautions

The following guidelines and precautions are provided for the user.

- Stacking: Certified values of thermal conductivity are valid for a single unit and are invalid for stacked units.
- Slicing: Certified values of thermal conductivity are invalid for a unit where the thickness of the material has been modified by slicing.
- Cutting: It is possible to cut the reference material unit into smaller pieces. It is imperative to verify that bulk density of each piece is within the certified range of bulk density (Sec.8.1)
- Compression: This SRM unit should not be compressed more than 3.5 % of original thickness considering the compressive resistance.
- Temperature Limit: A lower temperature limit for SRM 1453a has not been established but, the standard specification of EPS in use of thermal insulation indicates application temperatures from -54 °C to 74 °C [13]. The softening as a measure of the upper temperature limit is between 70 °C to 80 °C [14].

References

[1] ASTM International (2023) *ASTM C177-19e1 – Standard Test Method for Steady-State Heat Flux Measurements and Thermal Transmission Properties by Means of the Guarded-Hot-Plate Apparatus* (ASTM International, West Conshohocken, PA). https://doi.org/10.1520/C0177-19E01
[2] ASTM International (2021) *ASTM C518-21 – Standard Test Method for Steady-State Thermal Transmission Properties by Means of the Heat Flow Meter Apparatus* (ASTM International, West Conshohocken, PA). https://doi.org/10.1520/C0518-21
[3] Federal Trade Commission (2019) *R-value Rule 16 CFR Part 460 - Labeling and Advertising of Home Insulation (Electronic Code of Federal Regulations)*. https://federalregister.gov/a/05-10683
[4] Zarr RR, Pintar AL (2012) SRM 1453, Expanded Polystyrene Board, for Thermal Conductivity from 281 K to 313 K, *NIST Special Publication (SP) 260-175*. http://dx.doi.org/10.6028/NIST.SP.260-175
[5] Zarr RR, Harris AC, Roller JF (2011) Standard Reference Materials: SRM 1450d, Fibrous-Glass Board, for Thermal Conductivity from 280 K to 340 K, *NIST Special Publication (SP)* 260-173. https://doi.org/10.6028/NIST.SP.260-173
[6] Zarr RR, Heckert NA (2020) Certification of Standard Reference Material® 1450e Fibrous Glass Board, *NIST Special Pulication (SP) 260-201*. https://doi.org/10.6028/NIST.SP.260-201
[7] May W, Parris R, Beck C, Fassett J, Greenberg R, Guenther F, Kramer G, Wise S, Gills T, Colbert J (2000) Standard Reference Materials: Definitions of Terms and Modes Used at NIST for Value-Assignment of Reference materials for Chemical Measurements. *NIST Special Publication (SP) 260-136*. https://nvlpubs.nist.gov/nistpubs/Legacy/SP/nistspecialpublication260-136.pdf
[8] International Organization for Standardization (2015) *ISO Guide 30:2015 – Reference materials - Selected terms and definitions* (International Organization for Standardization, Geneva, Switzerland).
[9] ASTM International (2024) *ASTM C168-25 – Standard Terminology Relating to Thermal Insulation* (ASTM International, West Conshohocken, PA). https://doi.org/10.1520/C0168-25
[10] International Bureau of Weights and Measures (2008) *JCGM 100:2008 – Evaluation of measurement data - Guide to the expression of uncertainty in measurement* (Joint Committee for Guides in Metrology, International Bureau of Weights and Measures, Paris, France). https://doi.org/10.59161/JCGM100-2008E
[11] Taylor BN, Kuyatt CE (1994) *Guidelines for evaluating and expressing the uncertainty of NIST measurement results* (US Department of Commerce, Washington D.C. NIST Technical Note 1297). https://emtoolbox.nist.gov/Publications/NISTTechnicalNote1297s.pdf
[12] Zarr RR (2010) Assessment of uncertainties for the NIST 1016 mm guarded-hot-plate apparatus: extended analysis for low-density fibrous-glass thermal insulation. *Journal of research of the national institute of standards and technology* 115(1):23. https://nvlpubs.nist.gov/nistpubs/jres/115/1/V115.N01.A04.pdf
[13] ASTM International (2023) *ASTM C578-22 – Standard Specification for Rigid, Cellular Polystyrene Thermal Insulation* (ASTM International, West Conshohocken, PA). https://doi.org/10.1520/C0578-22

[14] Product Information Bulletin 306 (2018) Satety Data Sheet Plasti-Fab EPS products for construction applications. *Plasti-Fab EPS product solutions*. https://www.plastifab.com
[15] Doiron T, Stoup J (1997) Uncertainty and dimensional calibrations. *Journal of Research of the National Institute of Standards and Technology* 102(6):647. https://tsapps.nist.gov/publication/get_pdf.cfm?pub_id=820840
[16] Product Information Bulletin 248 (2019) PlastiSpan 40 Insulation Material Property Data. *Plasti-Fab EPS product solutions*. https://www.plastifab.com
[17] Roark RJ (1965) *Formulas for Stress and Strain. Fourth Edition* (McGraw-Hill Book Company, New York, N.Y.), 4th Ed.
[18] Rennex B (1983) Error analysis for the National Bureau of Standards 1016 mm guarded hot plate. *Journal of thermal insulation* 7(1):18-51.
[19] Hahn M (1974) Robinson line-heat-source guarded hot plate apparatus. *Heat Transmission Measurements in Thermal Insulations, ASTM STP* 544:167-192.
[20] ASTM International (2023) *ASTM C165-23 – Standard Test Method for Measuring Compressive Properties of Thermal Insulations* (ASTM International, West Conshohocken, PA,). https://doi.org/10.1520/C0165-23

Appendix 1 – Bulk Density Uncertainty

A1.1 Digital Balance Uncertainty

For a laboratory balance in a controlled environment, the combined standard uncertainty (k = 1), $\mu_{c,bal}$, is calculated using Eq. (A-1)

$$\mu_{c,bal} = 2\sqrt{\mu_s^2 + s_p^2} \qquad \text{(A-1)}$$

where μ_s is the standard uncertainty for the standard mass artifact; and s_p is the process standard deviation. For the 100 g, 200 g, 300 g mass standard artifacts used to check the balance, the standard uncertainties (μ_s) were obtained from the 2022 Troemner Calibration Certificate 220577411-2 to be 0.000 000 05 kg, 0.000 000 10 kg, and 0.000 000 15 kg , respectively. The maximum standard uncertainty among three mass artifacts, 0.000 000 15 kg, was taken as a conservative estimate for μ_s^2. As summing a uniform distribution, the process standard deviation (s_p) was determined from Eq. (A-2)

$$s_p = \frac{b}{\sqrt{3}} \qquad \text{(A-2)}$$

where b is equal to one display unit of the balance, For b equal to 0.0001 kg, s_p is equal to 0.000 058 kg. $\mu_{c,\ bal}$ was determined to be 0.0001 kg.

A1.2 Height Gage Uncertainty

The combined standard uncertainties of the electronic height gages, $\mu_{c,\ gage}$, were determined from Eq. (A-3)

$$\mu_{c,gage} = 2\sqrt{\mu_{s,block}^2 + s_p^2 + \mu_1^2 + \mu_2^2 + \mu_3^2} \qquad \text{(A-3)}$$

where $\mu_{s,\ block}$ is the standard uncertainty for the gage block. $s_{p,}$ is the standard uncertainty of the process (i.e. instrument uncertainty). μ_1 is the standard uncertainty of reference datum (i.e., granite surface plate). μ_2 is the standard uncertainty due to thermal expansion. μ_3 is the standard uncertainty due to elastic deformation of the insulation material.

Detailed description of the standard uncertainties for dimensional measurements are presented as follows:

- $\mu_{s,\ block}$: The gage blocks were calibrated between 2022 and 2023 by the NIST Dimensional Metrology Group (NIST Test No. 685-O-0000038571-22). The expanded uncertainty (k = 2) of the gage block for the thickness measurement was 0.0016 mm. The expanded uncertainty (k = 2) of both gage blocks (L4M041 and L4M042) for the length measurement were 0.00012 mm.

- s_p: The instrument uncertainties for the height gages were obtained from the manufacturer specification. The expanded uncertainties (k = 2) for the 300 mm and 610 mm height gages were ±0.025 mm and ±0.038 mm , respectively.
- μ_1: The flatness of the granite surface plate was assessed by LTI Metrology in 2022 (Calibration Certificate NIS001-22-04-01845-1). The overall flatness of the surface plate (48 W × 72L × 8H) was determined to be less than or equal to 0.036 mm, designated as a Grade B surface plate. For the thickness measurement, μ_1 was assumed to be zero because the height gage was stationary from its tare position.
- μ_2: The effect of thermal expansion on the gage blocks was determined by the equation of $\alpha(20°C - t)L_{block}$ with the recommended α values ($12{\times}10^{-6}$ °C^{-1} for $L_{block} < 100$ mm or $10.5{\times}10^{-6}$ °C^{-1} for $L_{block} > 500$ mm [15]) and the maximum surface plate temperature of 24.4 °C. $\mu_{2,\ thickness}$ and $\mu_{2,\ length}$ were -0.0008 mm and -0.0282 mm, respectively.
- μ_3: The effects due to elastic deformation of the materials were determined from the loading of the workpiece/touch probe (Fig. 2 and 3). The applied loading from the 32 mm dia. metal workpiece (36 g) and the measuring force of the touch probe were 0.35 N and 0.4 N, respectively. The contact pressure applied by the workpiece and probe was determined to be 936 Pa. Modulus was estimated to be 10.3 MPa using the material property data sheet [16], and resulted 0.01 % deformation (0.0013 mm) for the mean thickness (14.3 mm) as μ_3 under 936 Pa pressure.

Table A1.1 Uncertainty budget for dimensional measurements

Identifier	Description	Standard uncertainty (mm) , (k = 1)	
		Length (l_2), width (l_5)	Thickness (L)
$\mu_{s,\ block}$	Gage block #1 (thickness) Gage blocks #2 (L4M041 and L4M042 wrung together)	--- 0.000122	0.000815 ---
s_p	Height gage #1 (300 mm) Height gage #2 (610 mm)	--- 0.019	0.0125 ---
μ_1	Datum surface (granite plate)	0.0178	0
μ_2	Thermal expansion (24.4 °C)	-0.0282	-0.0008
μ_3	Elastic deformation of insulation	neglect	0.0013
$\mu_{c,\ gage}$	Combined standard uncertainty (k = 1)	0.077	0.025

A1.3 Dimensional Uncertainties

The combined standard uncertainties (k = 1) for the thickness and length-width were determined from Eq. A-4. In both cases, the standard uncertainties due to squareness and thickness variations were higher than the standard uncertainties associated with the measurement process.

$$\mu_c(L) = \sqrt{\mu_{c,gage\#1}^2 + \mu^2(L)} = \sqrt{0.025^2 + 0.078^2} = 0.082 \text{ mm} \quad \text{(A-4)}$$

$$\mu_c(l_2) = \mu_c(l_5) = \sqrt{\mu_{c,gage\#2}^2 + \mu^2(l)} = \sqrt{0.077^2 + 0.186^2} = 0.201 \text{ mm}$$

where $\mu(L)$ is the standard uncertainty of the pooled variance for the thickness measurements and $\mu(l)$ is the standard uncertainty of the pooled variance for the lateral dimensional measurements.

Appendix 2 – Uncertainty Analysis for Thermal Conductivity (λ)

A2.1 Background

NIST officially adopted a new policy [7] for the expression of measurement uncertainty consistent with international practices set for the in the ISO Guide to the Expression of Uncertainty in Measurement [10], also known as the "GUM".

The combined standard uncertainty of a measurement result, $u_c(y)$ is expressed as the positive square root of the combined variance $u_c^2(y)$:

$$u_c(y) = \sqrt{\sum_{i=1}^{N} c_i^2 u^2(x_i)} \qquad \text{(A-5)}$$

Each standard uncertainty, $u(x_i)$, is evaluated as either a Type A or Type B method. Type A standard uncertainties are evaluated by statistical means. The evaluation of uncertainty by means other than a statistical analysis of a series of observations is termed a Type B evaluation, which is usually based on a scientific judgement and may include measurement data from another experiment, experience, a calibration certificate, or manufacturer specification.

A2.2 Uncertainty for λ_{exp}

The standard uncertainty for λ_{exp} was evaluated based on the standard uncertainties for the specimen heat flow (Q), meter area (A), in-situ thickness (L), and specimen temperature difference (ΔT). These individual standard uncertainties were evaluated by either statistical methods (Type A), or other means (Type B).

A2.3 Specimen heat flow (Q)

Under normal operation, the guard plate and ambient air temperature were maintained such that lateral heat losses (Q_{gap} and Q_{edge}) were reduced to negligible proportions. Under these circumstances, the specimen heat flow (Q) was determined by measuring the direct current (DC) electrical power and voltage provided to the meter-plate heater (Q_m). The electrical circuit for the measurement consisted of a standard resistor, nominally 0.1Ω standard resistor placed in an oil bath at 25.00 °C in conjunction with series with the electrical heater of the meter area as illustrated in Fig. A2.1.

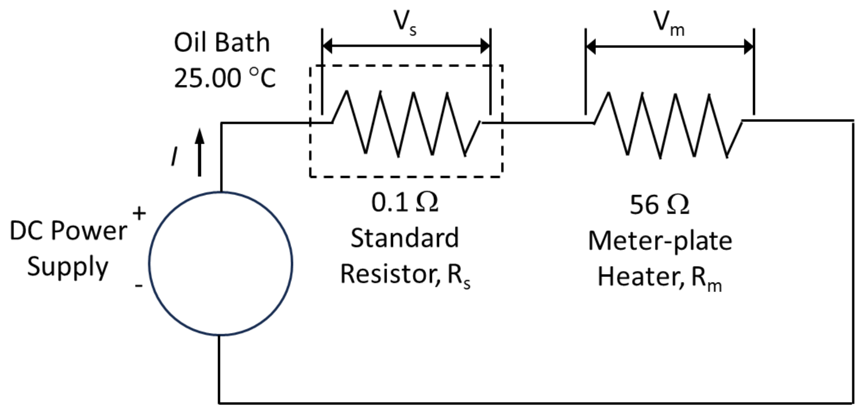

Figure A2.1. Electric schematic for the meter-plate power measurement

Equation A-6 defines Q_m.

$$Q_m = IV_m = \frac{V_s}{R_s} V_m \qquad \text{(A-6)}$$

where I is the current determined from the voltage drop (V_s) across the standard resistor and V_m is the voltage drop measured across the electrical leads to the meter plate.

A2.3.1 Combined Standard Uncertainty for Power Measurement (Q_m)

The contributory uncertainties for the standard uncertainties of Q_m include: 1) calibration of the standard resistor (type B evaluation); 2) platinum resistance thermometers (PRTs) self-heating (Type B evaluation); and 3) voltage measurements for V_s and V_m (Type A and Type B evaluations). The Type A standard uncertainty for Q_m was determined by pooling the standard deviations of repeated power measurements (n = 120) during a guard hot plate test, and the uncertainty estimates for $u(Q_m)_A$ is explained at the end of this section. The Type B standard uncertainty for Q_m with the contributor uncertainties in Eq. A-7 yields:

$$u_c(Q_m)_B = \sqrt{c_{V_s}^2 u^2(V_s)^2 + c_{R_s}^2 u^2(R_s)^2 + c_{V_m}^2 u^2(V_m)^2} \qquad \text{(A-7)}$$

where the sensitivity coefficient (c_i) are defined as follows:

$$c_{V_s} = \frac{\partial Q_m}{\partial V_s} = \frac{V_m}{R_s}$$
$$c_{R_s} = \frac{\partial Q_m}{\partial R_s} = -\frac{V_s V_m}{R_s^2}$$
$$c_{V_m} = \frac{\partial Q_m}{\partial V_m} = \frac{V_s}{R_s} = I$$

The input values for R_s and $u(R_s)$ in Eq. A-7 were 0.1000698 Ω and 0.000001 Ω (k = 1), respectively. The standard uncertainties for V_s and V_m are determined from Eq. A-8

$$u(V) = \frac{a}{\sqrt{3}} \qquad \text{(A-8)}$$

where a is the interval half-widths for V_s and V_m (300 mV and 30 V ranges, respectively) based on the 1-year manufacturer specification for the integrating voltmeter. a for V_s and V_m were computed from Eq. A-9a and A-9b respectively.

V_s, a = 0.00008 × *reading* + 8 μV + 0.0001 × *reading* (A-9a)
V_m: a = 0.00008 × *reading* + 300 μV + 0.0001 × *reading* (A-9b)

Table A2.1 summarized the standard uncertainty components for Q_m at T_m of 282 K, 298 K, 314 K.

Table A2.1 summary of the standard uncertainty components for $u(Q_m)$

T_m (K)	$u(Q_m)_A$ (W)	V_{std} (V)	$u(V_{std})$ (V)	V_m (V)	$u(V_m)$ (V)	$u_c(Q_m)_B$ (W)
282	0.00127	0.048	0.000 011 8	26.6	0.0029	0.0034
298	0.00148	0.049	0.000 013 1	27.3	0.0030	0.0039
314	0.00144	0.050	0.000 013 3	28.0	0.0031	0.0040

A2.3.2 Guard Imbalance (Q_{gap})

A heat flow, occurring as either a gain or loss, arises when the temperature of a thermal guard is imbalanced at the guard gap between the meter plate and guard plate and the heat loss at the edges of the specimens. The terms Q_{gap} and Q_{edge} represent both lateral heat loss at the guard gap between the meter plate and guard plate (Q_{gap}) and the heat loss at the edges of the specimens (Q_{edge}). Imbalance tests were conducted by creating temperature differences either across the guard gap (V_g) or the mean specimen temperature at the specimen edge and the ambient air temperature (T_a - T_m).

Table A2.2 summarizes an experimental design of the imbalance tests for two parameters (V_g and T_a – T_m). These parameters were varied for five test conditions. The last row in Table A2.2 is a center point, that is, a balanced test point where all imbalance settings were set equal to zero.

Table A2.2. The experimental design for imbalance tests with 2 factors

Index	V_g (μV)	T_a - T_m (K)
1	+50	+5
2	+50	-5
3	-50	+5
4	-50	-5
5	0	0

The test sequence shown in Table A2.3 was randomized for each level of T_m at 282 K, 298 K, 314 K (5+5+5 = 15 tests). The tests were conducted with one pair of specimens of expanded polystyrene boards (297, 054) installed in the guarded-hot-plate apparatus and encircled with fibrous polyester blanket insulation. The imbalance effect (ΔQ) on the power input to the meter plate (Q_m) in the steady-state was defined as:

$\Delta Q = Q_m - Q_{m0}$ (A-10)

where Q_{m0} is the power input to the meter-plate heater for balanced condition (i.e. V_g and $T_a - T_m$ were both set to zero).

Table A2.3 summarizes the test results from the imbalance tests at T_m of 282 K, 298 K, 314 K. The balanced conditions at multiple T_m were used to establish a baseline value for analyses of the data. Therefore, the response variable (y) and input variables (x_1, x_2) of the imbalance test results were normalized with respect to the balance tests. The data from Table A2.3 were fit to an empirical model for ΔQ given in Eq. A-11:

$y = \Delta Q = b_1 x_1 + b_2 x_2$ (A-11a)
$y = b_1 (V_g - V_{g0}) + b_2 [(T_a - T_m) - (T_a - T_m)_0]$ (A-11b)

The presence of an offset coefficient b_0 was initially considered for the model given in Eq. A-11b, however, the term was not included because the term is predicted to be nearly zero from theory [12].

Table A2.3. Imbalance test results in Yates order

Index	T_m (K)	ΔT (K)	$Y, (Q_m - Q_{m0})$ (W)	$X_1 (V_{gap} - V_{gap0})$ (μV)	$X_2, (T_a - T_m) - (T_{a0} - T_{m0})$ (K)
1	282	22.00	-0.1013	50.09	5.00
2	282	22.00	0.1192	-50.00	4.99
3	282	22.00	0.1128	-49.94	-4.98
4	282	22.00	-0.1092	49.98	-4.99
5	282	22.00	0.	0.	0.
1	298	22.00	0.1152	-49.96	5.00

2	298	22.01	-0.1159	49.99	5.00
3	298	22.00	-0.1300	50.00	-5.01
4	298	22.00	0.1023	-50.01	-5.00
5	298	22.00	0.	0.	0.
1	314	22.00	0.1239	-50.04	-5.00
2	314	22.00	-0.1164	49.98	-5.00
3	314	22.00	-0.1152	49.94	5.00
4	314	22.00	0.1290	-50.05	5.00
5	314	22.00	0.	0.	0.

Table A2.4 summarizes the parameter estimates and approximate standard deviations determined from multiple variable linear regression for coefficients b_1 and b_2 at T_m of 282 K, 298 K, and 314 K.

Table A2.4. Parameter estimates and standard deviations for b_1 and b_2 in Eq. (A1-11b)

T_m (K)	b_1 ($W \cdot \mu V^{-1}$)	*Std* (b_1) ($W \cdot \mu V^{-1}$)	b_2 ($W \cdot K^{-1}$)	*Std* (b_2) ($W \cdot K^{-1}$)
282	-0.002212	0.000063	0.000722	0.000632
298	-0.002317	0.000082	0.001353	0.000819
314	-0.002422	0.000061	0.000308	0.000614

Applying Eq. A-5 with Eq. A-11a yields

$$u_c\,(\Delta Q) = \sqrt{c_{b_1}^2 u^2(b_1) + c_{x_1}^2 u^2(x_1) + c_{b_2}^2 u^2(b_2) + c_{x_2}^2 u^2(x_2)} \qquad \text{(A-12)}$$

with

$$c_{a_i} = \frac{\partial(\Delta Q)}{\partial b_i} = x_i$$

$$c_{x_i} = \frac{\partial(\Delta Q)}{\partial x_i} = b_i$$

Table A2.5 summarizes the input values for Eq. A-12 and the corresponding estimates for $u_c(\Delta Q)$ at T_m of 282 K, 298 K, and 314 K. Under steady-state test conditions, the input estimates x_1 and x_2 are nearly zero.

Table A2.5. Estimates for $u_c(\Delta Q)$

T_m (K)	x_1 (μV)	$u(b_1)$ ($W \cdot \mu V^{-1}$)	b_1 ($W \cdot \mu V^{-1}$)	$u(x_1)$ (μV)	x_2 (K)	$u(b_2)$ ($W \cdot K^{-1}$)	b_2 ($W \cdot K^{-1}$)	$u(x_2)$ (K)	$u_c(\Delta Q)$ (W)
282	-0.0256	0.00072	-0.00221	2.42	0.0000	0.00063	0.00006	0.5	0.0054
282	-0.0263	0.00072	-0.00221	2.42	0.0007	0.00063	0.00006	0.5	0.0054

282	-0.0396	0.00072	-0.00221	2.42	0.0022	0.00063	0.00006	0.5	0.0054
298	-0.0041	0.00135	-0.00232	2.48	-0.0016	0.00082	0.00008	0.5	0.0057
298	0.0539	0.00135	-0.00232	2.48	0.0023	0.00082	0.00008	0.5	0.0057
298	-0.0328	0.00135	-0.00232	2.48	0.0002	0.00082	0.00008	0.5	0.0057
314	0.0233	0.00031	-0.00242	2.54	-0.0010	0.00061	0.00006	0.5	0.0061
314	0.0544	0.00031	-0.00242	2.54	0.0004	0.00061	0.00006	0.5	0.0061
314	0.0512	0.00031	-0.00242	2.54	0.0008	0.00061	0.00006	0.5	0.0061

A2.3.3 Combined Standard Uncertainty *u (Q)*

The combined standard uncertainty *u(Q)* was obtained from Eq. A-13.

$$u_c(Q) = \sqrt{u^2(Q_m)_A + u^2(Q_m)_B + u^2(\Delta Q)} \qquad \text{(A-13)}$$

where:
$u(Q_m)_A$ = standard uncertainty of repeated power measurements (n=120) during a test (W)
$u(Q_m)_B$ = standard uncertainty of the meter-plate power input (W)
$u_c(\Delta Q)$ = combined standard uncertainty for parasitic heat flows computed in Eq. A-12 (W)

Table A2.6 summarized the input values for Eq. A-13 and the corresponding estimates for $u_c(Q)$ at T_m of 282 K, 298 K, and 314 K.

Table A2.6. Combined standard uncertainty (k = 1) for $u_c(Q)$

T_m (K)	$u(Q_m)_A$ (W)	$u(Q_m)_B$ (W)	$u_c(\Delta Q)$ (W)	$u_c(Q)$ (W)	Q_{ave} / 2 (W)	$u_{c,\,rel}$ (Q) (%)
282	0.00127	0.0035	0.0054	0.0065	6.344	0.10 %
298	0.00148	0.0039	0.0057	0.0071	6.661	0.11 %
314	0.00144	0.0040	0.0061	0.0075	6.971	0.11 %

A2.4 Meter Area (A)

The meter area is the mathematical area through which the heat input to the meter plate (Q_m) flows normal to the heat flow direction under ideal guarding conditions (i.e., $Q_{gap} = Q_{edge} \equiv 0$) into the specimen. Note that the meter area is not the same as the area of the meter plate. The circular meter area was calculated from Eq. A-14 below:

$$A = \frac{\pi}{2}(r_0^2 + r_i^2)\left(1 + \alpha \Delta T_{mp}\right)^2 \qquad \text{(A-14)}$$

where:
r_0 = the outer radius of the meter plate (m);

r_i = the inner radius of the guard plate (m);
α = coefficient of thermal expansion of 6061-T6 aluminum (K^{-1})
ΔT_{mp} = temperature difference of the meter plate from ambient (K) (T_h – 20 °C)

A2.4.1 Plate Dimensions

Based on the check measurements using a coordinate measuring machine in 1994, the diameter of the meter plate was determined to be 405.67 mm, and a uniform gap width of 0.89 mm was achieved using the pin gauges. The uncertainty of the pin gauges was 0.005 mm / -0.000 mm. The input values for r_0 and r_i were determined to be 0.20282 m and 0.20373 m, respectively, and the standard uncertainty (k =1) for both input values was taken to be 0.0254 mm.

A2.4.2. Thermal expansion

An input value of 23.6 × 10^{-6} K^{-1} at 20 °C was taken as the coefficient of thermal expansion (α) from handbook data for aluminum alloy 6061-T6. The standard uncertainty (k =1) for the value of α was estimated conservatively to be 10 % (i.e., 2.36 × 10^{-6} K^{-1}).

A2.4.3 Combined standard uncertainty for $u_c(A)$

The application of Eq. A-5 to Eq. A-14 yields

$$u_c(A) = \sqrt{c_{r_0}^2 u^2(r_0) + c_{r_i}^2 u^2(r_i) + c_\alpha^2 u^2(\alpha) + c_{\Delta T_{mp}}^2 u^2(\Delta T_{mp})} \qquad \text{(A-15)}$$

with

$$c_{r_0} = \frac{\partial A}{\partial r_0} = \pi r_0 (1 + \alpha \Delta T_{mp})^2$$

$$c_{r_i} = \frac{\partial A}{\partial r_i} = \pi r_i (1 + \alpha \Delta T_{mp})^2$$

$$c_\alpha = \frac{\partial A}{\partial \alpha} = \pi \Delta T_{mp} (r_0^2 + r_i^2)(1 + \alpha \Delta T_{mp})$$

$$c_{\Delta T_{mp}} = \frac{\partial A}{\partial (\Delta T_{mp})} = \pi \alpha (r_0^2 + r_i^2)(1 + \alpha \Delta T_{mp})$$

Table A2.7 summarized the contributory uncertainties for calculating $u_c(A)$.

Table A2.7. Standard uncertainty components (k = 1) for A

	Description	Estimate	Standard uncertainty
$u_1(r_0)_B$	Meter-plate outer radius	202.82 mm	0.0254 mm
$u_2(r_i)_B$	Guard-plate inner radius	203.71 mm	0.0254 mm
$u_3(\alpha)_B$	Linear thermal expansion coefficient	2.36 × 10^{-5} K^{-1}	2.36 × 10^{-6} K^{-1}

$u_4(\Delta T_{mp})_B$	Temperature difference (T_m=282 K)	- 0.15 K	0.077 K
$u_4(\Delta T_{mp})_B$	Temperature difference (T_m=298 K)	15.85 K	0.077 K
$u_4(\Delta T_{mp})_B$	Temperature difference (T_m=314 K)	31.85 K	0.077 K

Table A2.8 summarizes the combined standard uncertainties of the meter area calculation, $u_c(A)$ at T_m of 282 K, 298 K, and 314 K.

Table A2.8. Combined standard uncertainty for $u_c(A)$

T_m (K)	A (m^2)	$u_c(A)$ (m^2)	$u_{c,\,rel}(A)$ (%)
282	0.12981	0.000023	0.018
298	0.12991	0.000025	0.019
314	0.13001	0.000030	0.023

A2.5 In-situ Thickness (*L*)

The thickness of each pair of specimens was measured during testing using the average of eight (four top and four bottom) linear positioning transducers at the periphery of the plates (approximately 90 ° intervals). Each device consists of a digital readout (resolution of 2.54×10^{-6} m) and a slider translating on a tape scale bonded to a precision ground plate of a low thermal expansion iron-nickel (FeNi36) alloy. The digital readouts are reset by placing four fused-quartz spacers on known thickness between the cold plate and hot plate.

The standard uncertainties associated with the eight linear positioning transducers were determined for each guarded hot plate test using the equation of $s/\sqrt{n}$ where *s* was the standard deviation of the digital readouts and *n* was equal to 8. The standard uncertainty $u(L)_A$ computed from the pooled experimental standard deviations for the 15 tests was found to be 0.0799 mm. Contributory uncertainty components for *L* are described below.

A2.5.1 Fused-quartz spacers for $u_1(L)_A$

The standard uncertainty computed from the pooled standard deviations of multiple measurement locations of the four fused-quartz spacer in the guarded hot plate was determined to be 0.0042 mm (k = 1).

A2.5.2 Linear Positioning System for $u_1(L)_B$

The standard uncertainty of four linear positioning transducers on the individual cold plates was based on the accuracy specification from the manufacturer as 0.0051 mm (k = 1) [12]. Since the individual transducers have the same accuracy specifications, the transducers on each cold plate have the same standard uncertainty ($u_1 = u_2 = u_3 = u_4 = u$ = 0.0029 mm) and sensitivity coefficient ($c_1 = c_2 = c_3 = c_4 = c = \partial y/\partial L$ = 1/4). Application of Eq. A-5, the combined standard uncertainty of the eight position transducers was determined to be 0.0021 mm.

A2.5.3 Micrometer for $u_2(L)_B$

The standard uncertainty for the micrometer used to determine the lengths of the fused quartz spacers was based on a uniform rectangular distribution with a symmetrical half-width *a* of 0.0025 mm. Substitution of the half-width using Eq. A-8 ($a/\sqrt{3}$, where *a* is the interval half-width) yields a standard uncertainty of 0.0015 mm (k = 1).

A.2.5.4 Repeatability of Linear Positioning System for $u_3(L)_A$

Table A2.9 summarize the short-term repeatability of the linear position transducers determined from a series of replicate measurements taken over four days using the fused-quartz spacers as reference values. For these measurements, the digital readouts were initially set to the length values of the individual fused-quartz spacers placed between the cold plate and hot plate. The cold plate was lifted from the spacers and subsequently lowered in contact with the spacers, and this procedure was repeated five times to check within-day variation (20 observations total for four days).

Table A2.9. Summary statistics for short-term repeatability of linear positioning system

Day	Replicates	Day average (mm)	Within-day standard deviation (mm)
1	5	12.665	0.003
2	5	12.671	0.001
3	5	12.671	0.002
4	5	12.668	0.001

A.2.5.5 Plate flatness for $u_4(L)_A$

Two contributory effects comprise the plate flatness: 1) multiple thickness observations of the meter plate (Type A evaluation), 2) coordinate measuring machine (CMM) uncertainty (Type B evaluation). The standard uncertainty associated with the mean of 32 thickness measurements of the meter plate was determined to be 0.0023 mm. The standard uncertainty of CMM was based on the accuracy specification from the manufacture as 0.0051 mm (k = 1). The combined standard uncertainty for the plate flatness was estimated from Eq. A-16 to be 0.0079 mm.

$$u_{c,4}(L)_A = \sqrt{2(u_A^2 + u_B^2)} \quad \text{(A-16)}$$

A.2.5.6 Plate Deflection for $u_5(L)_A$

The potential deflection of the cold plate under a mechanical load is evaluated as a Type B uncertainty using classical stress and strain formulae developed for flat plates. Clamping forces are transmitted axially by extension rod and distributed over a concentric circular attachment at the center of the cold plate. For a uniform load over the circular attachment with the radius (r_0), the maximum deflection (y_{max}) at the center of the cold plate is given the by following formula from Ref. [17].

$$u_5(L)_B = y_{max} = -\frac{3F(m^2-1)}{16\pi E m^2 t_c^3}\left[4r_0^2 \ln\frac{r_c}{r_0} + 2r_0^2\left(\frac{3m+1}{m+1}\right) + \frac{r_0^4}{r_c^2} - r_c^2\left(\frac{7m+3}{m+1}\right) + \frac{(r_c^2-r_0^2)r_0^4}{r_c^2 r_0^2}\right] \quad \text{(A-17)}$$

where:
F = applied load (N),
m = reciprocal of Poisson's ratio (dimensionless),
E = modulus of elasticity (N/m^2),
t_c = thickness of cold plate (m),
r_c = radius of cold plate (m)

The cold plate was fabricated from aluminum alloy 6061-T6 and the dimension are 1016 mm in diameter and 25.4 mm in thickness. The values for m, E, and r_c were taken to be $(0.33)^{-1}$ = 3.0, 6.89×10^7 kPa, and 508 mm, respectively. Substituting into Eq. A-17 yields a value of 0.0125 mm for y_{max} under a compression load of 189 N. Although this approach approximates the cold plate deflection, the uncertainty of the plate deflection depends on the plate design and the stiffness of the specimen, and the magnitude of the applied load. Considering these factors, the major limitation of this assessment on y_{max} is caused by the geometry of the cold plate because the cold plate is a combined structure with a channel for allowing the flow of coolant internally.

A.2.5.7 Combined Standard Uncertainty for $u_c(L)_A$

Table A2.10 summarizes the uncertainty components $u_i(L)$ with the evaluation method (Type A or B), source, and standard uncertainty. The component uncertainties are either test dependent ($u(L)$, spacer dependent ($u_1(L)$), process dependent ($u_3(L)$), apparatus depend ($u_4(L)$ and $u_5(L)$).

Table A2.10. Standard uncertainty components (k = 1) for L

Source	Description	Standard uncertainty (mm)
$u(L)_A$	In-situ thickness measurements	0.0799
$u_1(L)_A$	Fused-quartz spacers	0.0042
$u_1(L)_B$	System uncertainty of position transducers	0.0021

$u_2(L)_B$	Micrometer uncertainty	0.0015
$u_3(L)_A$	Short-term repeatability	0.0036
$u_4(L)_B$	Plate flatness	0.0079
$u_5(L)_B$	Plate deflection under load	0.0125

Eq. A-18 computes the combined standard uncertainty (*k* =1) for L.

$$u_c(L) = \sqrt{u^2(L) + u_1^2(L) + u_2^2(L) + u_3^2(L) + u_4^2(L) + u_5^2(L)} \qquad \text{(A-18)}$$

Substituting the standard uncertainty components from Table A2.10 into Eq. A-18 yields a combined standard uncertainty of 0.0815 mm. For the average L equal to 14.20 mm, $u_{c,\,rel}(L)$ was determined to be 0.57 %.

A.2.6 Temperature difference (*ΔT*)

The term, ΔT, is defined as the surface-to-surface temperature difference across the specimen pair where T_h is the temperature of the hot plate and T_{c1} and T_{c2} are the temperatures of the two cold plates, respectively. Under steady-state conditions showing $T_{c1} \approx T_{c2}$, ΔT is defined by Eq. A-19.

$$\Delta T = T_h - (T_{c1} + T_{c2}) / 2 = T_h - T_c \qquad \text{(A-19)}$$

The temperature difference across the specimen is determined by computing temporal averages of three small capsule PRTs (Minco, Model S1059). The temperature of the hot plate was measured using the PRT (an outer diameter of 3.2 mm) that is located at the periphery of the meter plate with the angular position of 291 degree relative to the entry of the meter heater leads. The temperature of the cold plate was measured using the PRT that was inserted at the 457 mm deep bored from the side of the plate.

A.2.6.1 Repeated Observations, $u(\Delta T)_A$

The electrical resistances of the PRTs were recorded every two minutes by an automated data acquisition system (n = 120). The standard uncertainty of the temperature difference was subsequently computed from the pooled standard deviations for the 15 tests and found to be 0.0003 K, which was neglected in comparison to other temperature uncertainty estimates.

A.2.6.2 Temperature Measurement Uncertainty Sources, $u(T)$

The contributory uncertainty sources for $u(T)$ includes: 1) PRT calibration, 2) curve fit of calibration data, 3) electrical resistance measurement of the PRT, 4) temperature rise of sensor due to PRT self-heating, 5) plate temperature variation in the radial dimension, 6) plate temperature variation in the axial dimension.

A.2.6.2.1 Calibration, $u_1(T)_A$

The PRTs for the two cold plates and hot plate were calibrated by the NIST thermodynamic metrology group with a standard platinum resistance thermometer at – 40 °C, 0 °C, 40 °C, 80 °C, and 120 °C in December 2015. All temperatures in the calibration were based on the International Temperature Scale of 1990 (ITS-90). The expanded uncertainty (k=2) with 0.0024 K at 80 °C from the test report (No.685/287693) was used for the uncertainty analysis. The standard uncertainty associated with the PRT calibrations was 0.0012 K (k = 1).

A.2.6.2.2 Regression uncertainty, $u_2(T)_A$

For each PRT, the individual observations in ohms (Ω) were converted to temperature using a curve fit to the calibration data mentioned above. The curve-fits were obtained using a statistical plotting package from NIST. The residual standard deviation for the fit of each set of calibration data was pooled and the resulting standard uncertainty was 0.0084 K. The degrees of freedom from the regression analyses were 3.

A.2.6.2.3 PRT Electrical Resistance Measurement, $u_3(T)_B$

The standard uncertainty for electrical resistance measurement of the PRT was based on the 1-year manufacturer specification for the integrating voltmeter. A uniform rectangular distribution was assumed for the accuracy specification with a symmetrical half-width d computed from Eq. (A-20) where reading is in ohms.

300 Ω Range: d = 0.00015 × reading + 8 mΩ + 0.0001 × reading (A-20)

For a reading of 131.561 Ω, $d_{300\Omega}$ is 0.041 Ω from Eq. A-22. Substituting 131.561 Ω ± 0.041 Ω/2 in the PRT calibration curve fit yields a corresponding temperature half-width of 0.105 K. Submitting the half-width of 0.105 K in $d/\sqrt{3}$ yields a standard uncertainty of 0.061 for the PRT measuring the hot plate temperature. Using the same calibration and uncertainty analyses, the standard uncertainties of both cold plate PRTs were determined to be 0.061 K. The pooled standard uncertainty of 3 PRTs was 0.0607 K.

A.2.6.2.4 PRT Self-heating, $u_4(T)_B$

PRT with 131.561 Ω dissipates about 0.000132 W for a 1 mA excitation current. For the meter plate PRT, a thin layer of thermally conductive silicone paste was applied to the sensor exterior to improve thermal contact. For the cold plate PRTs, the thermal conductance of the metal-to-air-to-metal inface between sensor and plate was estimated to be 0.058 W·K^{-1}. Thus, the temperature rise (0.000132 W / 0.058 W·K^{-1}) was 0.0023 K.

A.2.6.2.5 Radial plate temperature variation, $u_5(T)_B$

From previous measurements, [18], the temperature profiles of the meter plate were estimated using independent thermopiles placed between the plate surfaces and semi-rigid samples. An estimate for the radial temperature uncertainty was taken to be 0.015 K.

A.2.6.2.6 Axial plate temperature variation, $u_6(T)_B$

Analysis results published in Hahn et al. [19] showed that the differences between the temperature at the guard gap and the average surface temperature of the meter plate was less than 0.01 % for measuring typical insulations using the hot plate design similar to NIST 1016 mm GHP. Therefore, the uncertainty assessment was neglected in further analyses.

A.2.6.3 Combined Standard Uncertainty of Temperature measurement, $u_c(T)$

Table 2.12 summarizes the contributory standard uncertainty sources $u_i(T)$, their descriptions, and corresponding uncertainty estimates for the PRT temperature measurement.

Table A2.12. Standard uncertainty components for *T*

Source	Description	Standard uncertainty (K)
$u(T)_A$	Repeated observations	Negligible
$u_1(T)_B$	PRT calibration by NIST thermometry group	0.0024
$u_2(T)_A$	PRT calibration data curve fit	0.0084
$u_3(T)_B$	Electrical resistance measurement/conversion	0.0607
$u_4(T)_B$	Temperature rise due to PRT self-heating	0.0023
$u_5(T)_B$	Temperature variation - planar direction	0.0150
$u_6(T)_B$	Temperature variation - axial direction	Negligible

The combined standard uncertainty (*k* = 1) for the temperature measurement was computed in Eq. A-21,

$$u_c(T) = \sqrt{\left(u^2(T)_A + \sum_{i=1}^{6} u_i^2(T)\right)} \qquad \text{(A-21)}$$

Substituting the standard uncertainty components from Table A2.12 into Eq. A-21 yields the combined standard uncertainty of 0.063 K.

A.2.6.4 Combined Standard Uncertainty of temperature difference, $u_c(\Delta T)$

For a double-sided guarded-hot-plate test, the temperature difference (ΔT) across the specimen pair was determined from Eq. A-22,

$$\Delta T = T_h - \frac{T_{c1}}{2} - \frac{T_{c2}}{2} = T_h - T_c \quad \text{(A-22)}$$

Applying Eq. A-5 to Eq. A-22 and setting $u(T_h)=u(T_{c1})=u(T_{c2})=u(T)$ with sensitivity coefficients of c_h=1 and $c_{c1}=c_{c2}$= -0.5 yields

$$u_c(\Delta T) = \sqrt{\frac{3}{2} \times u_c^2(T)} = \sqrt{1.5 \times 0.063^2} = 0.077 \text{ K} \qquad \text{(A-23)}$$

For ΔT = 21.999 K used in this SRM work, $u_{c,\,rel}\,(\Delta T)$ was determined to be 0.35 %.

A2.7 Uncertainty assessment for λ_{exp}

For the multiplicative expression in Eq. (2), the relative combined standard uncertainty in λ_{exp} can be expressed as the relative uncertainties associated with each factor combined in quadrature.

$$u_{c,rel}(\lambda_{exp}) = \frac{u_c(\lambda_{exp})}{\lambda_{exp}} = \sqrt{\left(\frac{u(Q)}{Q}\right)^2 + \left(\frac{u(\Delta T)}{\Delta T}\right)^2 + \left(\frac{u(L)}{L}\right)^2 + \left(\frac{u(A)}{A}\right)^2} \qquad \text{(A-24)}$$

The standard uncertainties and input quantities used in Eq. (A-24) are listed in the sections of the individual uncertainty assessments. Adding the individual factors with 0.00102 (0.0065/6.3440) for $u_c(Q)/Q$, 0.00018 (2.29E-05/0.12981) for $u_c(A)/A$, 0.00576 (8.15E-5/0.01415) for $u_c(L)/L$, 0.00352 (0.077/22.00) for $u_c(\Delta T)/T$), the maximum $u_{c,rel}\,(\lambda_{exp})$ at T_m of 282 K was determined to be 0.0068 (0.68 %) as a conservative estimate, therefore, the expanded uncertainty (k = 2) for the measured thermal conductivities is equal to 1.36 %.

Appendix 3 - Compressive properties of Expanded Polystyrene Foam

The compressive properties of SRM 1453a were determined using a servo hydraulic testing machine under Procedure A of ASTM C165-23 [20]. The main purpose is to demonstrate a maximum pressure limit of SRM 1453a for users to avoid the yielding of the material with permanent compressive deformation. Seven cylindrical specimens with a nominal diameter of 100 mm and thickness of 13.8 mm were cut from Board 199 and conditioned in an environment of 24.7 °C $\pm$ 0.1 °C and 39.6 % $\pm$ 0.7 % relative humidity for approximately 4 days. Since compressive resistance relies on bulk density, the specimen with the lowest density range was measured to establish the low end of the compressive resistance of the SRM.
The compression loading was applied at the speed of 1 mm/min and load-displacement data were obtained at a rate of 1 per sec during tests. To construct a load-displacement curve, the straight portion of the curve was extended to the x-axis using a straightedge, which establishing a zero-deformation point. The compressive resistance (*S*) was calculated from:

$$S = W/A \qquad \text{(A-25)}$$

where:

W = load at any given deformation, N, and,
A = original area of specimen, m^2.

The compressive resistance for the specimens is summarized in Table A3.1. An average compressive resistance was 200.8 kPa at an average deformation of 3.5 %. All specimens showed non-linear behavior above this deformation.

Table A3.1. Compressive resistance of SRM 1453a, Expanded Polystyrene Board

ID	Bulk density ($kg \cdot m^{-3}$)	Undeformed area (m^2)	Deformation (mm)	Strain (%)	Load (N)	Compressive resistance (kPa)
1	44.82	0.0083	0.48	3.5	1637.5	198.0
2	44.59	0.0081	0.48	3.4	1645.2	203.2
3	44.58	0.0081	0.48	3.5	1640.1	203.3
4	44.63	0.0081	0.48	3.4	1620.5	200.6
5	44.12	0.0081	0.47	3.4	1497.3	185.2
6	45.06	0.0081	0.48	3.4	1653.1	204.9
7	45.32	0.0081	0.49	3.6	1713.2	210.5
Mean	44.73	0.0081	0.48	3.5	1629.6	200.8
Std. dev.	0.38	0.0001	0.01	0.1	65.2	7.9

The compressive resistance of SRM 1453a is many orders of magnitudes higher than the compression stress of the clamps, therefore, deformations of SRM 1453a during the hot plate tests were within the elastic regime. Compared to SRM 1453 with the mean compressive resistance of 304 kPa at the mean deformation of 0.34 mm, SRM 1453a exhibit higher ductility that is influenced by combinations of more porous surface structures and different internal structures.

Appendix 4 – Supplemental Thermal Conductivity Measurements

The surface of the previous SRM 1453 was polished to remove surface imprints from the molding process before measuring the thermal conductivity. To investigate an effect of specimen surface on thermal conductivity, Expanded Polystyrene boards produced in the same batch of SRM 1453a were polished using a belt polishing machine at NIST. The polished specimen pair with the average density of 47.3 kg·m^{-3} was selected because the density is similar with the SRM 1453a pair with the mid-density range (47.3 kg·m^{-3} versus 48.1 kg·m^{-3}). The differences of the thermal conductivity between the non-polished and polished specimens varied from 0.01 % to 0.4 % within the range of T_m used in the SRM 1453a measurements. Due to its small contribution, no further hot plate measurements with other density ranges were performed.

Table 4.1. Comparisons of thermal conductivity data between the non-polished and polished Expanded Polystyrene boards

T_m (K)	$Q/2_{\text{non-polished}}$ (W)	$Q/2_{\text{polished}}$ (W)	$L_{\text{non-polished}}$ (mm)	L_{polished} (mm)	$\lambda_{\text{non polished}}$ (W·m^{-1}·K^{-1})	$\lambda_{\text{polished}}$ (W·m^{-1}·K^{-1})	$\lambda_{\text{Diff.}}$ (%)
282	6.3	6.7	14.2	13.3	0.03142	0.03130	0.40
290	6.5	6.9	14.2	13.3	0.03225	0.03214	0.36
303	6.6	7.1	14.2	13.4	0.03306	0.03301	0.15
306	6.8	7.2	14.2	13.4	0.03387	0.03384	0.07
314	7.0	7.4	14.3	13.4	0.03467	0.03466	0.01

Appendix 5 – List of Symbols, Abbreviations, and Acronyms

Symbol/Acronym	Description (Units)
A	meter area (m^2)
ΔQ	change in meter-plate heater power due to imbalance condition expressed in Eq. (A-12)
A_s	area of the specimen (board) (m^2)
b_i	regression coefficients in Eq. (A-13b)
c_i	sensitivity coefficient for uncertainty analysis
d	half-width of uniform distribution
DMM	digital multimeter
I	electrical direct current (A)
ID	identification
E	modulus of elasticity ($N \cdot m^{-2}$)
F	clamping pressure applied to specimen by cold plate (Pa)
k	coverage factor for uncertainty (dimensionless)
l_i	linear dimensions (length, width) of insulation board (mm)
L	thickness of the guarded-hot-plate test specimen (mm)
$\bar{L}$	mean thickness of insulation board dimensions (mm)
m_0	mass of the specimen (kg)
P_a	chamber air pressure (Pa)
PRT	platinum resistance thermometer
Q	heat flow rate through meter area of guarded-hot-plate test specimen (W)
Q_{edge}	edge heat flow (W)
Q_{gap}	lateral (i.e., radial) heat flow rate across the guard gap (W)
Q_m	input power to meter-plate resistance heater (W)
Q_{m0}	input power to meter-plate resistance heater under balanced temperature condition (W)
q	heat flow rate through a surface of unit area perpendicular to the direction of heat flow ($W \cdot m^{-2}$)
r	radius of the round cylindrical sample
r_0	outer radius of meter plate (m)
r_i	inner radius of meter plate (m)
r_c	radius of cold plate (m)
R	thermal resistance ($m^2 \cdot K \cdot W^{-1}$)
RH	relative humidity of chamber air (%)
t_c	thickness of cold plate (m)
T	temperature (K)
T_a	chamber air temperature (K)
T_c	(mean) cold-plate temperature (K)
T_h	hot-plate temperature (K)
T_m	mean specimen temperature (K) = $(T_h + T_c)/2$

Symbol/Acronym	Description (Units)
u_c	combined standard uncertainty (*k* = 1)
$U_{c,r}$	relative combined standard uncertainty (*k* = 1)
U	expanded uncertainty (*k* = 2)
U_r	relative expanded uncertainty (*k* = 2)
V_g	voltage difference across guard gap thermopile (μV)
V_{g0}	voltage difference across guard gap thermopile under balanced condition (μV)
V_m	voltage difference across meter-plate heater (V)
V_s	voltage difference across standard resistor (V)
x_1	imbalance input variable in Eq. (A-11a)
x_2	imbalance input variable in Eq. (A-11a)
y	response variable for imbalance study
α	linear thermal expansion coefficient (K^{-1})
ΔQ	change in meter-plate heater power due to imbalance condition described in Eq. (A-12) (W)
ΔT	surface-to-surface temperature difference across specimen (K) = (T_h - T_c)
ΔT_{ave}	mean temperature difference in Eq. (14) (K)
ΔT_{mp}	temperature difference of the meter plate in Eq. (A-16) (K) = T_h - 20°C
λ	thermal conductivity ($W \cdot m^{-1} \cdot K^{-1}$)
λ_a or k_a	apparent thermal conductivity ($W \cdot m^{-1} \cdot K^{-1}$)
λ_{exp}	experimental thermal conductivity in Eq. (14) ($W \cdot m^{-1} \cdot K^{-1}$)
ρ	bulk density ($kg \cdot m^{-3}$)
ρ_s	bulk density of specimen board in Eq. (1) ($kg \cdot m^{-3}$)
Additional subscripts	
c1	top cold plate/specimen
c2	bottom cold plate/specimen
A	Type A standard uncertainty evaluation
B	Type B standard uncertainty evaluation
Additional superscript	
$\bar{}$	denote sample mean